

A Structurally Localized Ensemble Kalman Filtering Approach

Boujemaa Ait-El-Fquih and Ibrahim Hoteit

King Abdullah University of Science and Technology (KAUST), Thuwal, Saudi Arabia

Abstract

State-of-the-art ensemble Kalman filtering (EnKF) algorithms require incorporating localization techniques to cope with the rank deficiency and the inherited spurious correlations in their error covariance matrices. Localization techniques are mostly *ad-hoc*, based on some distances between the state and observation variables, requiring demanding manual tuning. This work introduces a new ensemble filtering approach, which is inherently localized, avoiding the need for any auxiliary localization technique. Instead of explicitly applying localization on ensembles, the idea is to first localize the continuous analysis probability density function (pdf) before ensemble sampling. The localization of the analysis pdf is performed through an approximation by a product of independent marginal pdfs corresponding to small partitions of the state vector, using the variational Bayesian optimization. These marginals are then sampled following stochastic EnKF and deterministic ensemble transform Kalman filtering (ETKF) procedures, using ensembles larger than the partitions' size. The resulting filters involve the same forecast steps as their standard EnKF and ETKF counterparts but different analysis steps, iteratively adjusting the EnKF and ETKF updates of each partition based on the ensemble means of the other partitions. Numerical experiments are conducted with the Lorenz-96 model under different scenarios to demonstrate the potential of the proposed filters. The new filters' performances are comparable to those of the EnKF and ETKF with already tuned localization, both in terms of computational burden and estimation accuracy.

Keywords: Data assimilation; EnKF; ETKF; Localization; Variational Bayes.

1 Introduction

Bayesian filtering methods, also known as sequential data assimilation methods, follow a probabilistic framework in which the underlying state estimation problem is split into successive cycles of alternating forecast and analysis steps (Künsch, 2001; Hoteit et al., 2018). The forecast step computes the forecast probability density function (pdf) of the current state given past observations, by integrating the previous analysis pdf with the state model. The forecast pdf is then updated in the analysis step with the incoming observation to obtain the analysis pdf of the state given all observations up to the current time instant. Such forecast and analysis pdfs can be, in theory, exactly evaluated using the famous Kalman filter (KF) in the particular case of linear-Gaussian state-space systems (Kalman, 1960; Anderson and Moore, 1979). In practice, however, the use of the KF is limited to relatively small systems, to avoid a prohibitive cost for the computation and storage of large error covariance matrices (e.g., Ait-El-Fquih and Hoteit,

Correspondence to: boujemaa.aitelfquih@gmail.com, ibrahim.hoteit@kaust.edu.sa

2022b). This makes it impossible the use of KF in realistic large-scale geophysical applications, which further involves nonlinear systems.

In nonlinear but small systems, good Monte Carlo approximations for the forecast and analysis distributions can be obtained using the particle filter (PF), a popular numerical filtering method which provides mathematically sound schemes with asymptotic convergence properties and ease of implementation (e.g., [Gordon et al., 1993](#); [Doucet et al., 2000](#)). The PF applicability is limited to small systems because of the exponential relationship between the state dimension and the number of particles that need to be generated to efficiently sample the state-space, the so-called curse of dimensionality issue ([Crisan and Doucet, 2002](#); [Snyder et al., 2008](#); [Hoteit et al., 2008](#)). Some improved variants of PF have been introduced in an attempt to address both nonlinear and large-dimensional aspects (e.g., [Ades and van Leeuwen, 2013](#); [Beskos et al., 2014](#); [Septier and Peters, 2015](#); [Ait-El-Fquih and Hoteit, 2016](#); [Poterjoy, 2016](#); [Potthast et al., 2019](#); [Mauro et al., 2022](#)). In parallel, a distinct class of Bayesian inference methods known as Particle Flow Filters, which do not rely on importance weighting, has demonstrated applicability to high-dimensional geophysical problems (e.g., [Pulido and van Leeuwen, 2019](#); [Hu and van Leeuwen, 2021](#); [Hu et al., 2024](#)). However, despite their better robustness to the curse of dimensionality compared to the original PF, these are not up to standard yet in operational geophysical applications.

To date, the golden standard in many geophysical applications is still the ensemble KF (EnKF), thanks to its non-intrusive formulation and ease of implementation, remarkable robustness and effectiveness, and reasonable computational requirements (see e.g., [Reichle et al., 2002](#); [Edwards et al., 2015](#); [Anderson et al., 2009](#); [Hoteit et al., 2015, 2018](#), and references therein). The EnKF provides Gaussian-based Monte Carlo approximations of the state forecast and analysis distributions by ensembles of random realizations, customarily called ensemble members ([Evensen, 1994, 2006](#); [Hoteit et al., 2015](#)). In an EnKF cycle, the forecast step integrates the (analysis) ensemble forward with the dynamical state model to obtain a forecast ensemble of the new state, and the analysis step computes an analysis ensemble of the same state from the resulting forecast ensemble using a KF-like update based on the incoming observation and the observation error model ([Hoteit et al., 2018](#)).

In its original form (hereafter referred to as the stochastic EnKF, SEnKF), it perturbs the observations stochastically before applying the KF update to each ensemble member (e.g., [Burgers et al., 1998](#); [Houtekamer and Mitchell, 1998](#); [Hoteit et al., 2015](#)). The perturbation of the observations guarantees an asymptotic matching of the covariance of the sampled analysis ensemble to that of the theoretical KF ([Burgers et al., 1998](#)). However, despite the remarkable performances shown by the stochastic SEnKF in many applications, it underestimates the covariance when the ensemble size is smaller than the rank of the observation noise ([Hoteit et al., 2015](#)). This phenomenon can be either i) mitigated through for instance incorporating in the SEnKF an *improved sampling scheme* as in [Evensen \(2004, 2009\)](#) or a so-called second-order resampling scheme as in [Hoteit et al. \(2015\)](#), or ii) fully avoided using a deterministic (square root) EnKF formulation. Indeed, the deterministic EnKFs avoid perturbing the observations and sample the analysis ensemble from an update of the mean and a square-root form of the covariance of the forecast ensemble exactly as in the KF, based on the actual observation (e.g., [Pham, 2001](#); [Bishop et al., 2001](#); [Hoteit et al., 2002](#); [Tippett et al., 2003](#); [Hunt et al., 2007](#); [Hoteit et al., 2015](#)). Several deterministic EnKFs are available in the literature, mainly differing in the form of the analysis covariance square-root and the way it is matched. The most popular with publicly available codes being the ensemble transform KF (ETKF) ([Bishop et al., 2001](#); [Wang et al., 2004](#); [Hunt et al., 2007](#)), the singular evolutive interpolated KF ([Pham, 2001](#); [Hoteit et al., 2002](#)), and the ensemble adjustment KF ([Anderson, 2001](#); [Anderson et al., 2009](#)).

The good performances shown by all stochastic and deterministic EnKFs in realistic applications would not be possible without accounting, in their implementation, for the inevitable sampling and systematic errors ([Whitaker et al., 2008](#); [Houtekamer and Mitchell, 2005](#)). Sam-

pling errors stem from the use of small ensembles (compared to the - large - state dimension) in order to limit the computational cost. Systematic errors encompass the uncertainties caused by other imperfections, namely, the poor knowledge of state and observation model error statistics, the inadequacy between the nonlinear character of the models and the Gaussian assumption made to derive the filters, etc (e.g., [Ait-El-Fquih and Hoteit, 2020](#), and references therein).

Omitting sampling and systematic errors limits the representativeness of the covariance of the filter forecast (background) ensemble; this results in a deficient rank, underestimated diagonal variances, and spurious off-diagonals (cross-variances). This significantly limits the ability of the filter to fit the observations and to produce meaningful state estimates ([Whitaker and Hamill, 2002](#); [Furrer and Bengtsson, 2007](#); [T. M. Hamill and et al., 2009](#); [Houtekamer and Zhang, 2016](#); [Hoteit et al., 2018](#)). Incorporating covariance inflation ([Anderson, 2001](#)) and localization ([Houtekamer and Mitchell, 1998](#); [Hamill et al., 2001](#)) techniques into the EnKFs remain the most popular among the many approaches that have been proposed to account for these errors and mitigate their effects. Inflation counteracts the problem of underestimation of forecast variance by artificially increasing the ensemble spread, either by a multiplicative factor (e.g. [Anderson and Anderson, 1999](#); [Anderson, 2007b](#); [Miyoshi, 2011](#)), or an additive factor (e.g. [Mitchell and Houtekamer, 2000](#); [Whitaker and Hamill, 2012](#)), among others. Localization imposes a decay on the cross-covariance terms with spatial distance, which helps mitigating the issues related to rank deficiency and overestimation of cross-covariances ([Houtekamer and Mitchell, 1998](#); [Hamill et al., 2001](#)).

Most localization techniques are based on some distances between the locations of state variables and observations, the most standard of which are *the local analysis* ([Houtekamer and Mitchell, 1998](#)) and *covariance localization* ([Hamill et al., 2001](#)) techniques. Local analysis updates each of the state variables using only the observations located in its neighbourhood, while the covariance localization applies a Schur product on the forecast covariance matrix using a tapering matrix ([Gaspari and Cohn, 1999](#)). Other physical distance-based localization methods have been proposed by for e.g. [Houtekamer and Mitchell \(2001\)](#); [Zhang and Oliver \(2010\)](#); [Fertig et al. \(2007\)](#); [Bishop and Hodyss \(2007\)](#). Further works have also been conducted to deal with the situations where some or all of the state and/or observation variables cannot be associated with physical locations (e.g. [Bocquet, 2016](#); [Bishop and Hodyss, 2007](#); [Anderson, 2007a](#); [De La Chevrotière and Harlim, 2017](#); [Luo et al., 2018](#)).

All EnKF localization schemes explicitly apply on ensembles (discrete distributions), i.e., one first derives the ensemble sampler of the continuous analysis pdf (i.e., the EnKF) then incorporates localization within it. Here, we reverse this order by first localizing the continuous analysis pdf then deriving ensemble samplers of the resulting localized pdf. The localization of the analysis pdf consists of approximating it with a product of separable (independent) marginals pdfs using the (functional) variational Bayesian (VB) optimization, i.e., according to the Kullback-Leibler divergence (KLD) minimization criterion ([Smidl and Quinn, 2006](#); [Blei et al., 2017](#); [Urozayev et al., 2022](#)). This amounts to removing posterior interdependencies between partitions of the state vector. We then sample the resulting marginal analysis densities according to SEnKF- and ETKF-like analysis steps, but any other sampling scheme could be also used. If the ensemble size is larger than the partitions' size, the proposed ensemble schemes should work without incorporating any additional localization scheme.

The proposed partitioned SEnKF (pSEnKF) and ETKF (pETKF) share the same forecast step as the standard SEnKF and ETKF, and have different analysis steps operating partition-wise in an iterative way. More specifically, once classical SEnKF (resp. classical ETKF) update is applied for all partitions; the resulting ensemble (resp. mean ensemble) of each partition is then iteratively adjusted/corrected based on the ensemble means of the other partitions. Such an adjustment compensates in some way for the posterior independence imposed between the state partitions.

The concept of state partitioning using the VB approach has been already adopted in the

linear-Gaussian framework, first in (Ait-El-Fquih and Hoteit, 2015) where an element-wise mean-field (diagonal posterior covariance) approximation to the KF has been proposed, then in (Ait-El-Fquih and Hoteit, 2022b) where the element-wise approximation is relaxed to allow for partition-wise mean-field (block-diagonal posterior covariance) approximation. The present work is an extension of this prior work to the more general nonlinear ensemble-like framework.

The remainder of the paper is organized as follows. Section 2 formulates the Bayesian filtering problem and reviews the standard SENKF and ETKF. Section 3 introduces the proposed localization approach of the continuous analysis pdf. Section 4 focuses on its SENKF- and ETKF-like sampling, and provides a thorough discussion on the resulting new localized filters. Section 5 presents and analyses the results of numerical experiments that were conducted with the Lorenz-96 model, before concluding with a summary and general discussion in Section 6.

2 Classical Ensemble Kalman Filtering: SENKF and ETKF

2.1 Problem formulation

Let $\mathbf{x} = \{\mathbf{x}_n\}_{n=0}^N$ and $\mathbf{y} = \{\mathbf{y}_n\}_{n=0}^N$, with $\mathbf{x}_n \in \mathbb{R}^{d_x}$ and $\mathbf{y}_n \in \mathbb{R}^{d_y}$, denote a discrete-time (unknown) state process and an observation process, respectively. In data assimilation, these processes are typically described according to a state-space system of the form:

$$\begin{cases} \mathbf{x}_n &= \mathcal{M}_{n-1}(\mathbf{x}_{n-1}) + \mathbf{u}_{n-1}, \\ \mathbf{y}_n &= \mathbf{H}_n \mathbf{x}_n + \mathbf{v}_n; \end{cases} \quad (1)$$

$\mathcal{M}_{n-1}(\cdot)$ being a (possibly nonlinear) dynamical operator integrating the state of the system from time t_{n-1} to t_n , and \mathbf{H}_n an observational operator at time t_n , assumed linear here for simplicity. The case of a nonlinear \mathbf{H}_n could be treated as usual in EnKFs (e.g., Liu et al., 2015). The state noise process, $\mathbf{u} = \{\mathbf{u}_n\}_n$, and the observation noise process, $\mathbf{v} = \{\mathbf{v}_n\}_n$, are assumed to be independent, jointly independent and independent of the initial state, \mathbf{x}_0 . The noises \mathbf{u}_n and \mathbf{v}_n are further assumed Gaussian with zero-means and covariances, \mathbf{Q}_n and \mathbf{R}_n , respectively.

The filtering problem refers to the (online) inference of the state \mathbf{x}_n from the available observations, $\mathcal{Y}_n = \{\mathbf{y}_0, \dots, \mathbf{y}_n\}$, and aims at seeking for the analysis pdf, $p_n(\mathbf{x}_n)$, i.e., the pdf of \mathbf{x}_n conditioned on \mathcal{Y}_n . When a point estimate is needed, the posterior mean (PM), i.e., the mean of $p_n(\mathbf{x}_n)$, is often chosen as it is the optimum solution according to several criteria including the mean-squared error (MSE) minimization (van Trees, 1968).

The aforementioned independence assumptions enables a *recursive* calculation of $p_n(\mathbf{x}_n)$, driven by the state transition pdf,

$$p(\mathbf{x}_n | \mathbf{x}_{n-1}) = \mathcal{N}_{\mathbf{x}_n}(\mathcal{M}_{n-1}(\mathbf{x}_{n-1}), \mathbf{Q}_{n-1}), \quad (2)$$

and the likelihood pdf¹,

$$p(\mathbf{y}_n | \mathbf{x}_n) = \mathcal{N}_{\mathbf{y}_n}(\mathbf{H}_n \mathbf{x}_n, \mathbf{R}_n); \quad (3)$$

$\mathcal{N}_{\mathbf{x}}(\mathbf{m}, \mathbf{C})$ denotes a Gaussian pdf² of argument \mathbf{x} and parameters (\mathbf{m}, \mathbf{C}) (e.g., Künsch, 2001; Ait-El-Fquih and Desbouvries, 2006). An $(n-1, n)$ assimilation cycle (recursion) proceeds typically³ with a forecast step which uses the transition pdf to obtain the forecast pdf, $p_{n-1}(\mathbf{x}_n)$,

¹It is worth recalling that the term “likelihood” corresponds to $p(\mathbf{y}_n | \mathbf{x}_n)$ when \mathbf{y}_n is a fixed value, i.e., the value of the conditional pdf $p(\mathbf{y}_n | \mathbf{x}_n)$ at a given point \mathbf{y}_n . However, in this paper, we tolerate, as commonly done, some flexibility and attribute “likelihood” to $p(\mathbf{y}_n | \mathbf{x}_n)$ whether or not \mathbf{y}_n is fixed.

²The Gaussian forms (2) and (3) are immediate results of the Gaussian assumptions made on the noises \mathbf{u}_{n-1} and \mathbf{v}_n , respectively.

³A different filtering approach, involving the one-step-ahead smoothing pdf, can be found in Ait-El-Fquih and Hoteit (2022a) and references therein.

from the previous analysis pdf as,

$$p_{n-1}(\mathbf{x}_n) = \int p(\mathbf{x}_n|\mathbf{x}_{n-1})p_{n-1}(\mathbf{x}_{n-1})d\mathbf{x}_{n-1}, \quad (4)$$

followed by an analysis step which uses the likelihood to obtain the analysis pdf of the current state following Bayes' rule,

$$p_n(\mathbf{x}_n) \propto p(\mathbf{y}_n|\mathbf{x}_n)p_{n-1}(\mathbf{x}_n). \quad (5)$$

2.2 Ensemble Gaussian filtering: SEnKF and ETKF

The SEnKF and ETKF are Gaussian-based Monte Carlo implementations of the generic filtering algorithm (4)-(5), introduced to avoid the linearization of the models and to efficiently handle large-dimensional systems (Hoteit et al., 2018). They have been demonstrated to provide robust PM estimates even when they are implemented with small ensembles (Hoteit et al., 2015).

Both filters involve the same forecast step, as a Monte Carlo implementation of Eq. (4), producing a state forecast ensemble, $\{\mathbf{f}_n^{(m)}\}_{m=1}^M$, after propagating the previous analysis ensemble, $\{\mathbf{a}_{n-1}^{(m)}\}_{m=1}^M$, by the state model, i.e.,

$$\mathbf{f}_n^{(m)} = \mathcal{M}_{n-1}(\mathbf{a}_{n-1}^{(m)}) + \mathbf{u}_{n-1}^{(m)}, \quad m = 1, \dots, M; \quad (6)$$

$\mathbf{u}_{n-1}^{(m)}$ being a sample of the Gaussian model error pdf $\mathcal{N}(\mathbf{0}, \mathbf{Q}_{n-1})$.

Given the forecast ensemble and a new observation \mathbf{y}_n , the SEnKF and ETKF analysis steps are then derived under the assumption of Gaussian⁴ $p(\mathbf{x}_n, \mathbf{y}_n|\mathcal{Y}_{n-1})$, to restrict the problem to a Kalman-like linear update. SEnKF and ETKF have been respectively classified as stochastic and deterministic samplers of the same analysis density, $p_n(\mathbf{x}_n)$, based on the generic update step (5).

2.2.1 The (stochastic) SEnKF analysis step

The SEnKF analysis step uses perturbations $\mathbf{y}_n^{(m)}$ of the observation by adding random observational errors $\mathbf{v}_n^{(m)} \sim \mathcal{N}(\mathbf{0}, \mathbf{R}_n)$, i.e., $\mathbf{y}_n^{(m)} = \mathbf{y}_n + \mathbf{v}_n^{(m)}$, to update the forecast members according to the KF update step to obtain the analysis ensemble members:

$$\mathbf{a}_n^{(m)} = \mathbf{f}_n^{(m)} + \mathbf{K}_n(\mathbf{y}_n^{(m)} - \mathbf{H}_n\mathbf{f}_n^{(m)}), \quad m = 1, \dots, M. \quad (7)$$

The Kalman gain \mathbf{K}_n , which is a Monte Carlo approximation of $\text{cov}[\mathbf{x}_n, \mathbf{z}_n|\mathcal{Y}_{n-1}] \times (\text{cov}[\mathbf{z}_n|\mathcal{Y}_{n-1}] + \text{cov}[\mathbf{v}_n])^{-1}$ with $\mathbf{z}_n = \mathbf{H}_n\mathbf{x}_n$, can be expressed as:

$$\mathbf{K}_n = \mathbf{S}_{\mathbf{f}_n} \tilde{\mathbf{S}}_{\mathbf{f}_n}^T \left[\tilde{\mathbf{S}}_{\mathbf{f}_n} \tilde{\mathbf{S}}_{\mathbf{f}_n}^T + \mathbf{R}_n \right]^{-1}, \quad (8)$$

where $\mathbf{S}_{\mathbf{f}_n}$ denotes the forecast perturbation matrix (i.e., a square-root of the forecast sample error covariance) and $\tilde{\mathbf{S}}_{\mathbf{f}_n} = \mathbf{H}_n\mathbf{S}_{\mathbf{f}_n}$.

It is important to highlight a theoretical distinction regarding the stochastic update mechanism. While the standard formulation presented above involves perturbing the observation vector (Burgers et al., 1998), a rigorous derivation of the stochastic filter from the Bayesian standpoint reveals that the random perturbations should structurally be applied to $\mathbf{H}_n\mathbf{f}_n^{(m)}$, rather than to the observation (van Leeuwen, 2020; Ait-El-Fquih and Hoteit, 2022a), which leads to involve $-\mathbf{v}_n^{(m)}$ in Eq. (7) instead of $+\mathbf{v}_n^{(m)}$. Nevertheless, observing that both $+\mathbf{v}_n^{(m)}$ and $-\mathbf{v}_n^{(m)}$ are samples of the same *symmetric* Gaussian distribution, $\mathcal{N}(\mathbf{0}, \mathbf{R}_n)$, we tolerate, as customarily done, some flexibility in the present work and use $+\mathbf{v}_n^{(m)}$ instead.

⁴Note that since in system (1) the observation model is linear with a Gaussian noise, one only needs to assume the forecast pdf $p_{n-1}(\mathbf{x}_n)$ Gaussian, as it implies that $p(\mathbf{x}_n, \mathbf{y}_n|\mathcal{Y}_{n-1})$ is Gaussian.

2.2.2 The (deterministic) ETKF analysis step

Unlike the SEnKF analysis step, the ETKF analysis step is deterministic in the sense that it directly uses the observation to update the mean, $\hat{\mathbf{f}}_n$, of the forecast members and their perturbation matrix, $\mathbf{S}_{\mathbf{f}_n}$, based on the KF update step. The resulting analysis mean, $\hat{\mathbf{a}}_n$, and analysis perturbation matrix, $\mathbf{S}_{\mathbf{a}_n}$ (i.e., a square-root of the analysis sample error covariance), are then used to sample the analysis ensemble deterministically following a matching procedure of the first two moments of the KF solution (see e.g., Bishop et al., 2001; Tippett et al., 2003; Hoteit et al., 2015; Raboudi et al., 2019). Formally:

- $\hat{\mathbf{a}}_n$ results from a KF update of $\hat{\mathbf{f}}_n$ based on \mathbf{y}_n as,

$$\hat{\mathbf{a}}_n = \hat{\mathbf{f}}_n + \mathbf{K}_n(\mathbf{y}_n - \mathbf{H}_n\hat{\mathbf{f}}_n); \quad (9)$$

- $\mathbf{S}_{\mathbf{a}_n}$ is obtained from a transformation of $\mathbf{S}_{\mathbf{f}_n}$ according to the KF update of the covariance as,

$$\mathbf{S}_{\mathbf{a}_n} = \mathbf{S}_{\mathbf{f}_n} \mathbf{T}_n \mathbf{\Omega}_n; \quad (10)$$

\mathbf{T}_n being a square-root of $\mathbb{I}_M + \tilde{\mathbf{S}}_{\mathbf{f}_n}^T \mathbf{R}_n^{-1} \tilde{\mathbf{S}}_{\mathbf{f}_n}$, and $\mathbf{\Omega}_n$ is a centring matrix guaranteeing the second moment matching (i.e., it ensures that $\mathbf{S}_{\mathbf{a}_n} \mathbf{S}_{\mathbf{a}_n}^T$ matches the theoretical expression of the analysis covariance of the KF). Expressions of \mathbf{T}_n and $\mathbf{\Omega}_n$ can be found e.g., in Bishop et al. (2001); Pham (2001); Wang et al. (2004).

- The analysis members are finally sampled as,

$$\mathbf{a}_n^{(m)} = \hat{\mathbf{a}}_n + \sqrt{M-1}(\mathbf{S}_{\mathbf{a}_n})_m; \quad m = 1, \dots, M, \quad (11)$$

with $(\mathbf{S}_{\mathbf{a}_n})_m$ denotes the m -th column of $\mathbf{S}_{\mathbf{a}_n}$.

3 Localization of the theoretical analysis pdf

Let the state vector, \mathbf{x}_n , be split into K partitions, $\mathbf{x}_n^1, \mathbf{x}_n^2, \dots, \mathbf{x}_n^K$ of the same dimension, $d_p = d_x/K$. In the more general case where the partitions $\{\mathbf{x}_n^k\}_k$ have different dimensions $\{d_{p^k}\}_k$, the proposed schemes remain valid by only replacing Kd_p with $\sum_{k=1}^K d_{p^k}$. The analysis pdf, $p_n(\mathbf{x}_n)$, can be localized by dropping dependencies between its K marginals. Specifically, this can be achieved by approximating $p_n(\mathbf{x}_n)$ with a product of separable marginal pdfs⁵,

$$\begin{aligned} p_n(\mathbf{x}_n) &\approx \pi_n(\mathbf{x}_n) \\ &= \pi_n(\mathbf{x}_n^1) \pi_n(\mathbf{x}_n^2) \cdots \pi_n(\mathbf{x}_n^K). \end{aligned} \quad (12)$$

We adopt the VB approach and seek for the best approximation $\pi_n(\mathbf{x}_n)$, in the sense of KLD minimization or equivalently negative free energy (NFE) maximization (e.g., Fraysse and Rodet, 2014, and references therein), i.e.,

$$\pi_n(\mathbf{x}_n) = \arg \max_{q \in \Omega} \mathbb{E}_{q(\mathbf{x}_n)} \left[\ln \frac{p(\mathbf{x}_n, \mathbf{y}_n | \mathcal{Y}_{n-1})}{q(\mathbf{x}_n)} \right], \quad (13)$$

where Ω denotes a space of separable pdfs satisfying $q(\mathbf{x}_n) = \prod_{k=1}^K q(\mathbf{x}_n^k)$, and $\mathbb{E}_{q(\mathbf{x}_n)}[\cdot]$ the expected value with respect to (w.r.t.) $q(\mathbf{x}_n)$. Applying variational calculus to maximization (13) readily results in a solution $\pi_n(\mathbf{x}_n)$ whose marginals satisfy:

$$\pi_n(\mathbf{x}_n^k) \propto \mathcal{L}_{\mathbf{y}_n}(\mathbf{x}_n^k) \times \pi_{n-1}(\mathbf{x}_n^k), \quad (14)$$

⁵The same notation, $\pi(\cdot)$, will be used for the pdf of the whole vector, \mathbf{x}_n , and of those of partitions, \mathbf{x}_n^k

with,

$$\mathcal{L}_{\mathbf{y}_n}(\mathbf{x}_n^k) \propto \exp\left(\mathbb{E}_{\pi_n(\mathbf{x}_n^{k-})}[\ln p(\mathbf{y}_n|\mathbf{x}_n)]\right), \quad (15)$$

$$\pi_{n-1}(\mathbf{x}_n^k) \propto \exp\left(\mathbb{E}_{\pi_n(\mathbf{x}_n^{k-})}[\ln p_{n-1}(\mathbf{x}_n)]\right), \quad (16)$$

where $k = 1, \dots, K$ and \mathbf{x}_n^{k-} denotes the complement of \mathbf{x}_n^k in \mathbf{x}_n (Smidl and Quinn, 2008).

Eqs. (14)-(16) suggest that the proposed approach imposes independencies between $\pi_n(\mathbf{x}_n^k)$ and $\pi_n(\mathbf{x}_n^{k-}) = \prod_{j \neq k} \pi_n(\mathbf{x}_n^j)$ through ‘‘an averaging’’ of the log likelihood $\ln p(\mathbf{y}_n|\mathbf{x}_n)$ and the log forecast $\ln p_{n-1}(\mathbf{x}_n)$ w.r.t. $\pi_n(\mathbf{x}_n^{k-})$. In other words, for each $k = 1, \dots, K$, the partition \mathbf{x}_n^k of the full state, \mathbf{x}_n , is not localized by crudely ignoring the other partitions, \mathbf{x}_n^{k-} , but by ‘‘freezing’’ them by means of the aforementioned ‘‘averaging’’. On the other hand, one can notice that the K Eqs. (14) have the form of a Bayesian update step, linking priors $\pi_{n-1}(\mathbf{x}_n^k)$ with posteriors $\pi_n(\mathbf{x}_n^k)$ using likelihoods $\mathcal{L}_{\mathbf{y}_n}(\mathbf{x}_n^k)$.

Connection between the expression of the true analysis pdf $p_n(\mathbf{x}_n^k)$ (i.e., marginal of $p_n(\mathbf{x}_n)$) and that of its VB estimate, $\pi_n(\mathbf{x}_n^k)$, can be then made by rewriting $p_n(\mathbf{x}_n^k)$ in a similar functional form as $\pi_n(\mathbf{x}_n^k)$ (Eqs. (14)-(16)). This is achieved by applying the logarithm function on both sides of Eq. (5), taking the expectation w.r.t. $p_n(\mathbf{x}_n^{k-})$, and finally applying the exponential function. This yields:

$$p_n(\mathbf{x}_n^k) \propto \frac{\kappa_{\mathbf{y}_n}(\mathbf{x}_n^k) \times \tilde{p}_{n-1}(\mathbf{x}_n^k)}{\exp\left(\mathbb{E}_{p_n(\mathbf{x}_n^{k-})}[\ln p(\mathbf{x}_n^k|\mathbf{x}_n^k, \mathcal{Y}_n)]\right)}, \quad (17)$$

with,

$$\kappa_{\mathbf{y}_n}(\mathbf{x}_n^k) \propto \exp\left(\mathbb{E}_{p_n(\mathbf{x}_n^{k-})}[\ln p(\mathbf{y}_n|\mathbf{x}_n)]\right), \quad (18)$$

$$\tilde{p}_{n-1}(\mathbf{x}_n^k) \propto \exp\left(\mathbb{E}_{p_n(\mathbf{x}_n^{k-})}[\ln p_{n-1}(\mathbf{x}_n)]\right). \quad (19)$$

Now, given that Eqs. (18)-(19) are similar to Eqs. (15)-(16), the expression (17) of $p_n(\mathbf{x}_n^k)$ ends up with an extra term dependent on \mathbf{x}_n^k , $T_{\mathbf{y}_n}(\mathbf{x}_n^k) = \exp\left(\mathbb{E}_{p_n(\mathbf{x}_n^{k-})}[\ln p(\mathbf{x}_n^k|\mathbf{x}_n^k, \mathcal{Y}_n)]\right)$, compared to the expression (14) of $\pi_n(\mathbf{x}_n^k)$. In the particular case where the partitions are by essence independent conditionally on \mathcal{Y}_n , this extra term vanishes (as it becomes independent of \mathbf{x}_n^k) and expressions (14) and (17) coincide (i.e., $\mathcal{L}_{\mathbf{y}_n}(\mathbf{x}_n^k) = \kappa_{\mathbf{y}_n}(\mathbf{x}_n^k)$, $\pi_{n-1}(\mathbf{x}_n^k) = \tilde{p}_{n-1}(\mathbf{x}_n^k)$ and $\pi_n(\mathbf{x}_n^k) = p_n(\mathbf{x}_n^k)$). Such a scenario corresponds to state-space systems that do not involve connections between the different partitions (as if one has K independent systems, one for each partition). This is a very restrictive condition, that is not generally fulfilled in real-world applications.

In standard systems (i.e., in which state partitions connect with each other), the VB approach eliminates the term $T_{\mathbf{y}_n}(\mathbf{x}_n^k)$ (to make expressions (14) and (17) identical) by approximating it with a constant quantity, independent of \mathbf{x}_n^k , which is then included in the normalization term of Bayes’ formula (14). One can show that this approximation is performed as an ‘‘averaging’’ w.r.t. $p_n(\mathbf{x}_n^k)$, i.e.,

$$\begin{aligned} \pi_n(\mathbf{x}_n^k) &\stackrel{(14)}{\propto} \frac{\mathcal{L}_{\mathbf{y}_n}(\mathbf{x}_n^k) \times \pi_{n-1}(\mathbf{x}_n^k)}{\int_{\mathbb{R}^{d_p}} \mathcal{L}_{\mathbf{y}_n}(\mathbf{x}_n^k) \times \pi_{n-1}(\mathbf{x}_n^k) d\mathbf{x}_n^k}, \\ &\propto \frac{\mathcal{L}_{\mathbf{y}_n}(\mathbf{x}_n^k) \times \pi_{n-1}(\mathbf{x}_n^k)}{\mathbb{E}_{p_n(\mathbf{x}_n^k)}[\tilde{T}_{\mathbf{y}_n}(\mathbf{x}_n^k)]}, \end{aligned} \quad (20)$$

$\tilde{T}_{\mathbf{y}_n}(\mathbf{x}_n^k) = \exp\left(\mathbb{E}_{\pi_n(\mathbf{x}_n^{k-})}[\ln p(\mathbf{x}_n^k|\mathbf{x}_n^k, \mathcal{Y}_n)]\right)$. This means that to provide a separable KLD estimation to the analysis pdf, the VB approach modifies the standard (true) Bayesian approach by ‘‘freezing’’ the K terms $T_{\mathbf{y}_n}(\mathbf{x}_n^k)$ by means of ‘‘an averaging’’ over \mathbf{x}_n^k .

Finally, it is worth noting that in a Gaussian framework, the VB approach does not impose block diagonal structure to the true posterior pdf, but rather seeks to find the Gaussian pdf with block diagonal covariance that is closest (in the sense of criterion (13)) to the true posterior pdf. As such, even with the separable approximation (12) that implies block-diagonal covariance matrix in a Gaussian framework, the true posterior pdf does not necessarily have a block-diagonal covariance.

3.1 Calculation of the localized analysis pdfs $\pi_n(\mathbf{x}_n^k)$

As discussed above, although the VB marginal analysis pdfs, $\pi_n(\mathbf{x}_n^k)$, are, by construction, mutually independent, each of them is still related to a functional form involving the expectation w.r.t. the others, $\pi_n(\mathbf{x}_n^{k-})$. Such a functional relationship compensates for the enforced posterior independencies between the state partitions, a key advantage of the VB approach. However, it also has the drawback of precluding an exact evaluation of the K solutions (14) and approximations should therefore be performed.

One natural way to do so is to proceed with (coordinate descent-like) iterations (e.g., Bertsekas, 1995). That is, at iteration i , update successively each of the K marginals $\pi_n^i(\mathbf{x}_n^k)$ using the newly updated $\pi_n(\mathbf{x}_n^{k-})$. In that respect, the update (14) at iteration i reads:

$$\pi_n^i(\mathbf{x}_n^k) \propto \mathcal{L}_{\mathbf{y}_n}^i(\mathbf{x}_n^k) \times \pi_{n-1}^i(\mathbf{x}_n^k), \quad (21)$$

where $\mathcal{L}_{\mathbf{y}_n}^i(\mathbf{x}_n^k)$ and $\pi_{n-1}^i(\mathbf{x}_n^k)$ are respectively given by (15) and (16) using $\pi_n^{(i,i-1)}(\mathbf{x}_n^{k-}) = \prod_{j=1}^{k-1} \pi_n^i(\mathbf{x}_n^j) \times \prod_{j=k+1}^K \pi_n^{i-1}(\mathbf{x}_n^j)$ in the expectation operator (recall that $\pi_n(\mathbf{x}_n^{k-}) = \prod_{j=1}^{k-1} \pi_n(\mathbf{x}_n^j) \times \prod_{j=k+1}^K \pi_n(\mathbf{x}_n^j)$).

3.2 The generic localized filtering algorithm

Here, we present the forecast and analysis steps of the generic localized filtering algorithm for System (1). Denote hereafter \mathbf{H}_n^k and \mathbf{H}_n^{k-} the partitions of \mathbf{H}_n corresponding to the positions k and $k-$, respectively, i.e., satisfying $\mathbf{H}_n \mathbf{x}_n = \mathbf{H}_n^k \mathbf{x}_n^k + \mathbf{H}_n^{k-} \mathbf{x}_n^{k-}$. Let also $(\hat{\mathbf{x}}_{n|n-1}, \mathbf{P}_{n|n-1})$ the first two moments of the forecast pdf $p_{n-1}(\mathbf{x}_n)$, and $(\mathbf{m}_{n|j}^{k,i}, \mathbf{C}_{n|j}^k)$ the first two moments of $\pi_j^i(\mathbf{x}_n^k)$ with $j = n-1, n$ (we show in the Appendix that the covariances $\mathbf{C}_{n|j}^k$ are invariant over the iterations).

- *Forecast step.* $p_{n-1}(\mathbf{x}_n)$ is calculated from $\pi_{n-1}(\mathbf{x}_{n-1})$ following the standard forecast step, i.e., following Eq. (4) using $\pi_{n-1}(\mathbf{x}_{n-1})$ instead of $p_{n-1}(\mathbf{x}_{n-1})$.

- *Analysis step.* The resulting forecast pdf, $p_{n-1}(\mathbf{x}_n)$, is updated based on the newly acquired observation, \mathbf{y}_n , following an iterative procedure to obtain a localized analysis pdf, $\pi_n(\mathbf{x}_n)$. Starting from an initialization $\pi_n^0(\mathbf{x}_n) = p_{n-1}(\mathbf{x}_n)$, the i -th iteration calculates the marginals $\pi_n^i(\mathbf{x}_n^k)$ successively from $k = 1$ to K in three steps:

1. A first step computes the VB likelihood $\mathcal{L}_{\mathbf{y}_n}^i(\mathbf{x}_n^k)$ based on Eq. (15) using $\pi_n^{(i,i-1)}(\mathbf{x}_n^{k-})$ in the expectation operator. One obtains,

$$\mathcal{L}_{\mathbf{y}_n}^i(\mathbf{x}_n^k) = \mathcal{N}_{\mathbf{y}_n}(\mathbf{H}_n^k \mathbf{x}_n^k + \mathbf{H}_n^{k-} \mathbf{m}_{n|n}^{k-,i}, \mathbf{R}_n); \quad (22)$$

$$\mathbf{m}_{n|n}^{k-,i} = (\mathbf{m}_{n|n}^{1,i}, \dots, \mathbf{m}_{n|n}^{k-1,i}, \mathbf{m}_{n|n}^{k+1,i-1}, \dots, \mathbf{m}_{n|n}^{K,i-1}).$$

2. A second step applies ‘‘an adjustment’’ to the forecast $p_{n-1}(\mathbf{x}_n)$ according to Eq. (16) using $\pi_n^{(i,i-1)}(\mathbf{x}_n^{k-})$ in the expectation operator, to obtain $\pi_{n-1}^i(\mathbf{x}_n^k)$. Assuming that $p_{n-1}(\mathbf{x}_n)$ is

Gaussian, one obtains,

$$\pi_{n-1}^i(\mathbf{x}_n^k) = \mathcal{N}_{\mathbf{x}_n^k}(\mathbf{m}_{n|n-1}^{k,i}, \mathbf{C}_{n|n-1}^k); \quad (23)$$

$$\mathbf{m}_{n|n-1}^{k,i} = \hat{\mathbf{x}}_{n|n-1}^k + \mathbf{G}_n^k(\mathbf{m}_{n|n-1}^{k-,i} - \hat{\mathbf{x}}_{n|n-1}^{k-}), \quad (24)$$

$$\mathbf{C}_{n|n-1}^k = \mathbf{P}_{n|n-1}^k - \mathbf{G}_n^k \mathbf{P}_{n|n-1}^{k-,k}, \quad (25)$$

with $\mathbf{G}_n^k = \mathbf{P}_{n|n-1}^{k,k-}(\mathbf{P}_{n|n-1}^{k-})^+$, where $(\cdot)^+$ denotes the pseudo-inverse, and the covariances $\mathbf{P}_{n|n-1}^k$ and $\mathbf{P}_{n|n-1}^{k-}$ and the cross-covariances $\mathbf{P}_{n|n-1}^{k,k-}$ and $\mathbf{P}_{n|n-1}^{k-,k}$ are extracted from $\mathbf{P}_{n|n-1}$ according to the positions k and k^- .

3. The third step combines the Gaussian VB likelihood (22) with the Gaussian VB forecast (23)-(25) according to the Bayesian update (21), to obtain a Gaussian VB analysis pdf:

$$\pi_n^i(\mathbf{x}_n^k) = \mathcal{N}_{\mathbf{x}_n^k}(\mathbf{m}_{n|n}^{k,i}, \mathbf{C}_{n|n}^k); \quad (26)$$

$$\mathbf{m}_{n|n}^{k,i} = \mathbf{m}_{n|n-1}^{k,i} + \mathbf{L}_n^k(\mathbf{y}_n - \mathbf{H}_n^k \mathbf{m}_{n|n-1}^{k,i} - \mathbf{H}_n^{k-} \mathbf{m}_{n|n}^{k-,i}), \quad (27)$$

$$\mathbf{C}_{n|n}^k = \mathbf{C}_{n|n-1}^k - \mathbf{L}_n^k \mathbf{H}_n^k (\mathbf{C}_{n|n-1}^k)^T, \quad (28)$$

with $\mathbf{L}_n^k = \mathbf{C}_{n|n-1}^k (\mathbf{H}_n^k)^T [\mathbf{H}_n^k \mathbf{C}_{n|n-1}^k (\mathbf{H}_n^k)^T + \mathbf{R}_n]^{-1}$.

At convergence (last iteration, $i = I$), $\pi_n(\mathbf{x}_n^k) = \pi_n^I(\mathbf{x}_n^k)$ for all k .

4 Practical implementation: The partitioned-SEnKF (pSEnKF) and -ETKF (pETKF)

Here, we focus on SEnKF- and ETKF-like ensemble implementations of the generic algorithm presented in Section 3.2. For simplicity, we use the same notations used in Section 2 for the ensembles and their corresponding moments (sample means, sample covariances and perturbation matrices).

The filters pSEnKF and pETKF share the same forecast step as their standard counterparts (Eq. (6)). The derivation of their analysis steps based on the generic KF-like updates ((24)-(25), (27)-(28)) may involve computational challenges related to the gain matrices \mathbf{G}_n^k . Indeed, in an ensemble setting, these matrices can be computed based on the forecast perturbation matrices as,

$$\begin{aligned} \mathbf{G}_n^k &\approx \mathbf{S}_{\mathbf{f}_n^k} \mathbf{S}_{\mathbf{f}_n^{k-}}^T (\mathbf{S}_{\mathbf{f}_n^k} - \mathbf{S}_{\mathbf{f}_n^{k-}}^T)^+, \\ &= \mathbf{S}_{\mathbf{f}_n^k} (\mathbf{S}_{\mathbf{f}_n^{k-}})^+. \end{aligned} \quad (29)$$

In this localized setting, this requires a beforehand computation of K ($M \times (d_x - d_p)$)-sized pseudo-inverses, followed by K products (29), in addition to the need for storing the K computed $(d_p \times (d_x - d_p))$ -sized \mathbf{G}_n^k matrices during all iterations, as they are needed in the update (24) at every iteration. This can quickly become cumbersome when dealing with large-dimensional systems. This is dealt with in this preliminary work by simply ignoring the terms involving \mathbf{G}_n^k in Eqs. (24)-(25), reducing them to:

$$\mathbf{m}_{n|n-1}^{k,i} = \hat{\mathbf{x}}_{n|n-1}^k \quad \text{and} \quad \mathbf{C}_{n|n-1}^k = \mathbf{P}_{n|n-1}^k, \quad (30)$$

which in turns reduces the VB analysis updates (27)-(28) into,

$$\begin{aligned} \mathbf{m}_{n|n}^{k,i} &= \hat{\mathbf{x}}_{n|n-1}^k + \mathbf{L}_n^k(\mathbf{y}_n - \mathbf{H}_n^k \hat{\mathbf{x}}_{n|n-1}^k - \mathbf{H}_n^{k-} \mathbf{m}_{n|n}^{k-,i}), \\ &= \underbrace{\hat{\mathbf{x}}_{n|n-1}^k + \mathbf{L}_n^k(\mathbf{y}_n - \mathbf{H}_n^k \hat{\mathbf{x}}_{n|n-1}^k)}_{\Theta_n^k \text{ (classical KF)}} - \underbrace{\mathbf{L}_n^k \mathbf{H}_n^{k-} \mathbf{m}_{n|n}^{k-,i}}_{\text{adjustment}}, \end{aligned} \quad (31)$$

$$\mathbf{C}_{n|n}^k = \mathbf{P}_{n|n-1}^k - \mathbf{L}_n^k \mathbf{H}_n^k (\mathbf{P}_{n|n-1}^k)^T. \quad (32)$$

Under the Gaussian assumption on $p_{n-1}(\mathbf{x}_n)$, ignoring \mathbf{G}_n^k in Eqs. (24)-(25) amounts to ignoring the dependencies between \mathbf{x}_n^k and \mathbf{x}_n^{k-} conditionally on \mathcal{Y}_{n-1} , i.e., to assuming,

$$p(\mathbf{x}_n^k | \mathbf{x}_n^{k-}, \mathcal{Y}_{n-1}) = p_{n-1}(\mathbf{x}_n^k). \quad (33)$$

Noticing that this assumption leads to ignore the forecast cross-covariance across partitions, it can be interpreted as an implicit localization of the forecast distribution.

Eq. (31) suggests that at a given iteration, the VB analysis mean of a state partition, \mathbf{x}_n^k , is none other than a classical KF analysis mean, Θ_n^k , adjusted with a shift by a linear combination of the most recent values of the VB analysis means of the remaining partitions, \mathbf{x}_n^{k-} . Furthermore, Θ_n^k is computed only once, as it does not depend on iterations; this means that the iterative update (31) of the VB KF analysis mean, $\mathbf{m}_{n|n}^k$, is simply an iterative adjustment of the classical KF analysis mean, Θ_n^k , based on a linear combination of the most recent $\mathbf{m}_{n|n}^{k-}$.

4.1 The pSenKF analysis step

The pSenKF analysis step is an ensemble form of the iterative VB analysis step (31). That is, for each k -th partition, a classical SenKF update is first performed to obtain an ensemble $\{\boldsymbol{\theta}_n^{k,(m)}\}_{m=1}^M$, which is then adjusted iteratively with a shift by a linear combination of the most recent sample means $\hat{\mathbf{a}}_n^{k-}$, to obtain the VB analysis ensemble of interest, $\{\mathbf{a}_n^{k,(m)}\}_{m=1}^M$.

By analogy with the expression of Θ_n^k in Eq. (31) (and with Eqs. (7)-(8)), the classical SenKF update reads for $k = 1, \dots, K$,

$$\tilde{\mathbf{L}}_n^k = \mathbf{S}_{\mathbf{f}_n^k} \tilde{\mathbf{S}}_{\mathbf{f}_n^k}^T [\tilde{\mathbf{S}}_{\mathbf{f}_n^k} \tilde{\mathbf{S}}_{\mathbf{f}_n^k}^T + \mathbf{R}_n]^{-1}, \quad (34)$$

$$\boldsymbol{\theta}_n^{k,(m)} = \mathbf{f}_n^{k,(m)} + \tilde{\mathbf{L}}_n^k (\mathbf{y}_n^{(m)} - \mathbf{H}_n^k \mathbf{f}_n^{k,(m)}), \quad (35)$$

with $\tilde{\mathbf{S}}_{\mathbf{f}_n^k} = \mathbf{H}_n^k \mathbf{S}_{\mathbf{f}_n^k}$, $\mathbf{y}_n^{(m)} = \mathbf{y}_n + \mathbf{v}_n^{(m)}$ and $\mathbf{v}_n^{(m)} \sim \mathcal{N}(\mathbf{0}, \mathbf{R}_n)$. The iterations are then triggered. At iteration i , the VB analysis ensemble, $\{\mathbf{a}_n^{k,(m),i}\}_{m=1}^M$, is computed via an adjustment of the obtained $\{\boldsymbol{\theta}_n^{k,(m)}\}_{m=1}^M$ with a shift by $-\tilde{\mathbf{L}}_n^k \mathbf{H}_n^{k-} \hat{\mathbf{a}}_n^{k-,i}$, where the sample mean $\hat{\mathbf{a}}_n^{k-,i}$ is given as, $\hat{\mathbf{a}}_n^{k-,i} = (\hat{\mathbf{a}}_n^{1,i}, \dots, \hat{\mathbf{a}}_n^{k-1,i}, \hat{\mathbf{a}}_n^{k+1,i-1}, \dots, \hat{\mathbf{a}}_n^{K,i-1})$. Specifically, at iteration i , one has for $k = 1, \dots, K$:

$$\mathbf{a}_n^{k,(m),i} = \boldsymbol{\theta}_n^{k,(m)} - \tilde{\mathbf{L}}_n^k \mathbf{H}_n^{k-} \hat{\mathbf{a}}_n^{k-,i}; \quad m = 1, \dots, M. \quad (36)$$

At convergence (last iteration I), $\{\mathbf{a}_n^{k,(m)}\}_{m=1}^M = \{\mathbf{a}_n^{k,(m),I}\}_{m=1}^M$ and $\hat{\mathbf{a}}_n^k = \hat{\mathbf{a}}_n^{k,I}$ for all k . Convergence is assumed to be reached if, for instance, a predefined maximum number of iterations, I , is exceeded, or if an error based on the difference between two successive $\hat{\mathbf{a}}_n = (\hat{\mathbf{a}}_n^1, \dots, \hat{\mathbf{a}}_n^K)$ (i.e., based on $\hat{\mathbf{a}}_n^i - \hat{\mathbf{a}}_n^{i-1}$) become less than a given threshold.

An $(n-1, n)$ assimilation cycle of the pSenKF is outlined in Algorithm 1. The computational load is further discussed in Section 4.3.

4.2 The pETKF analysis step

The pETKF analysis step is derived based on the KF-like Eqs. (31)-(32) following the principle of ETKF (Section 2.2.2), i.e., “the moments” $\hat{\mathbf{a}}_n$ and $\mathbf{S}_{\mathbf{a}_n}$ are first computed partition-wise then used to sample the members $\mathbf{a}_n^{(m)}$.

The analysis means, $\hat{\mathbf{a}}_n$, are computed following the iterative KF adjustment procedure (31). That is, for each k -th partition, a classical KF update is first performed to obtain an analysis mean, $\hat{\boldsymbol{\theta}}_n^k$, which is then adjusted iteratively, based on a linear combination of the most recent $\hat{\mathbf{a}}_n^{k-}$, to obtain the VB analysis mean of interest, $\hat{\mathbf{a}}_n^k$.

By analogy with the expression of Θ_n^k in Eq. (31), the classical KF update reads for $k = 1, \dots, K$,

$$\hat{\boldsymbol{\theta}}_n^k = \hat{\mathbf{f}}_n^k + \tilde{\mathbf{L}}_n^k (\mathbf{y}_n - \mathbf{H}_n^k \hat{\mathbf{f}}_n^k). \quad (37)$$

Algorithm 1: pSEnKF

- Forecast: Sample the ensemble $\{\mathbf{f}_n^{(m)}\}_{m=1}^M$ using Eq. (6), then inflate it before computing $\hat{\mathbf{f}}_n$ and $\mathbf{S}_{\mathbf{f}_n}$.
- Analysis:
 - 1) Classical SEEnKF: For $k = 1, \dots, K$, compute $\tilde{\mathbf{L}}_n^k$ using Eq. (34) then $\{\boldsymbol{\theta}_n^{k,(m)}\}_{m=1}^M$ using Eq. (35).
 - 2) Iterative adjustment:
 - ▷ Initialize $\hat{\mathbf{a}}_n = \hat{\mathbf{f}}_n$ and $\mathbf{h}_n = \mathbf{H}_n \hat{\mathbf{f}}_n$.
 - ▷ **While not converged do:** for $k = 1, \dots, K$,

$$\begin{aligned}
 \mathbf{h}_n &= \mathbf{h}_n - \mathbf{H}_n^k \hat{\mathbf{a}}_n^k \\
 \mathbf{a}_n^{k,(m)} &= \boldsymbol{\theta}_n^{k,(m)} - \tilde{\mathbf{L}}_n^k \mathbf{h}_n; \quad m = 1, \dots, M \\
 \hat{\mathbf{a}}_n^k &= \frac{1}{M} \sum_{m=1}^M \mathbf{a}_n^{k,(m)} \\
 \mathbf{h}_n &= \mathbf{h}_n + \mathbf{H}_n^k \hat{\mathbf{a}}_n^k
 \end{aligned}$$

End

At iteration i , the VB analysis mean, $\hat{\mathbf{a}}_n^{k,i}$, is computed via an adjustment of the obtained $\hat{\boldsymbol{\theta}}_n^k$ with a shift by $-\tilde{\mathbf{L}}_n^k \mathbf{H}_n^{k-} \hat{\mathbf{a}}_n^{k-,i}$:

$$\hat{\mathbf{a}}_n^{k,i} = \hat{\boldsymbol{\theta}}_n^k - \tilde{\mathbf{L}}_n^k \mathbf{H}_n^{k-} \hat{\mathbf{a}}_n^{k-,i}. \quad (38)$$

The iteration loop is terminated following the same stopping criterion discussed in pSEnKF. Assuming convergence is reached after I iterations, one takes $\hat{\mathbf{a}}_n^k = \hat{\mathbf{a}}_n^{k,I}$ for all k .

Square-roots of the sample analysis covariances are computed based on Eq. (32) in a similar way to Eq. (10) as,

$$\mathbf{S}_{\mathbf{a}_n^k} = \mathbf{S}_{\mathbf{f}_n^k} \mathbf{T}_n^k \boldsymbol{\Omega}_n, \quad (39)$$

where the transformation matrices, \mathbf{T}_n^k , are here given by square roots of $\mathbb{I}_M + \tilde{\mathbf{S}}_{\mathbf{f}_n^k}^T \mathbf{R}_n^{-1} \tilde{\mathbf{S}}_{\mathbf{f}_n^k}$.

The resulting $\{\hat{\mathbf{a}}_n^k\}_{k=1}^K$ and $\{\mathbf{S}_{\mathbf{a}_n^k}\}_{k=1}^K$ are then concatenated column-wise to respectively form $\hat{\mathbf{a}}_n$ and $\mathbf{S}_{\mathbf{a}_n}$, based on which the analysis members, $\mathbf{a}_n^{(m)}$, are sampled as in Eq. (11).

An $(n-1, n)$ assimilation cycle of the pETKF is summarized in Algorithm 2, and the computational load is discussed in Section 4.3.

4.3 Discussion

The proposed generic filtering scheme in Section 3.2 shares the same forecast step as the standard generic filtering algorithm (Eq. (4)), but involves a different analysis step that operates partition-wise by splitting the state \mathbf{x}_n into low-dimensional sub-states, \mathbf{x}_n^k , $k = 1, \dots, K$, following the VB approach. Such an analysis step is endowed with an iterative procedure; each iteration, i , consists of K successive Bayesian update steps linking respectively the K state-partitions \mathbf{x}_n^k to the observation \mathbf{y}_n , in order to compute the VB analysis pdfs $\pi_n^i(\mathbf{x}_n^k)$.

In the particular case where the observation model is linear, such K Bayesian updates reduce to K KF-like updates computing means and covariances of the pdfs $\pi_n^i(\mathbf{x}_n^k)$. The covariances of $\pi_n^i(\mathbf{x}_n^k)$ do not depend on the iterations and are thus computed once, outside of the iteration loop, using the classical KF update applied on the models $\mathbf{y}_n = \mathbf{H}_n^k \mathbf{x}_n^k + \mathbf{v}_n$. The mean of each of the $\pi_n^i(\mathbf{x}_n^k)$ varies with the iterations as an iterative adjustment of the classical KF analysis mean (i.e., obtained from applying KF on the model $\mathbf{y}_n = \mathbf{H}_n^k \mathbf{x}_n^k + \mathbf{v}_n$), with a shift by a linear

Algorithm 2: pETKF

- Forecast: Sample the ensemble $\{\mathbf{f}_n^{(m)}\}_{m=1}^M$ using Eq. (6), then inflate it before computing $\hat{\mathbf{f}}_n$ and $\mathbf{S}_{\mathbf{f}_n}$.
 - Analysis:
 - 1) Mean:
 - ▷ Classical KF: For $k = 1, \dots, K$, Compute $\tilde{\mathbf{L}}_n^k$ using Eq. (34), then $\hat{\boldsymbol{\theta}}_n^k$ using Eq. (37).
 - ▷ Iterative Adjustment:
 - ◇ Initialize $\hat{\mathbf{a}}_n = \hat{\mathbf{f}}_n$ and $\mathbf{h}_n = \mathbf{H}_n \hat{\mathbf{f}}_n$.
 - ◇ **While not converged do:** for $k = 1, \dots, K$,
$$\begin{aligned} \mathbf{h}_n &= \mathbf{h}_n - \mathbf{H}_n^k \hat{\mathbf{a}}_n^k \\ \hat{\mathbf{a}}_n^k &= \hat{\boldsymbol{\theta}}_n^k - \tilde{\mathbf{L}}_n^k \mathbf{h}_n \\ \mathbf{h}_n &= \mathbf{h}_n + \mathbf{H}_n^k \hat{\mathbf{a}}_n^k \end{aligned}$$
- End**
- 2) Covariance square-root: For $k = 1, \dots, K$, compute $\mathbf{S}_{\mathbf{a}_n^k}$ from $\mathbf{S}_{\mathbf{f}_n^k}$ using Eq. (39).
 - 3) Members: Sample the ensemble $\{\mathbf{a}_n^{(m)}\}_{m=1}^M$ following Eq. (11) based on the resulting $\hat{\mathbf{a}}_n$ and $\mathbf{S}_{\mathbf{a}_n}$.
-

combination of the most recent values of the means that correspond to the remaining partitions, \mathbf{x}_n^{k-} .

The proposed pSEnKF and pETKF algorithms are ensemble variants of the afore-described generic filtering algorithm, under the Gaussian assumption on the forecast pdf and the independence assumption (33). They share the same forecast step with the standard SEEnKF and ETKF filters, but involve different analysis steps that are respectively stochastic and deterministic ensemble forms of the afore-described iterative generic analysis step. More specifically, the pSEnKF analysis step consists of an iterative SEEnKF adjustment procedure based on linear combinations of sample analysis means (i.e., adjustments of ensembles generated by the standard SEEnKF analysis), whereas the pETKF analysis step employs exactly the above generic iterative KF adjustment procedure before (deterministically) generating the analysis ensembles.

Splitting the state vector into partitions could be seen as an intrinsic localization, negating the need for (external) auxiliary localization, most notably when the ensemble size, M , is larger than the partitions' size, d_p . In fact, unlike the SEEnKF and ETKF, in which the localization is applied on discrete distributions, i.e., on (forecast or analysis) ensembles, the proposed approach starts by applying localization on the (continuous) analysis density, based on the VB approach, then sampling the resulting localized pdf by pSEnKF and pETKF algorithms without equipping them with any (external) localization, subject that $M > d_p$.

It is also worth noting that the aforementioned (in Section 3.1) functional relationship that links each VB analysis pdf $\pi_n^i(\mathbf{x}_n^k)$ to expectation w.r.t. $\pi_n^{(i,i-1)}(\mathbf{x}_n^{k-})$, appears in the pSEnKF and pETKF analysis steps under the form of a correction term, $-\tilde{\mathbf{L}}_n^k \mathbf{H}_n^{k-} \hat{\mathbf{a}}_n^{k-,i}$ (i.e., Eqs. (36) and (38)). This means that contrary to what one might expect, the partitioning that is applied on the (continuous) analysis pdf using the VB approach does not make the analysis pSEnKF and pETKF ensembles completely independent between the partitions, as these are still linked via their sample means, i.e., $\{\mathbf{a}_n^{k,(m),i}\}_m$ are linked to $\hat{\mathbf{a}}_n^{k-,i}$. More precisely, this coupling acts at the mean estimate level but does not reintroduce full cross-partition (analysis) covariances.

As a result, when the true posterior exhibits strong dependencies across partition boundaries (i.e., when boundaries split strongly coupled neighbors), the analysis update may preserve these couplings reasonably well in the ensemble mean (through the iterative mean correction), while cross-boundary correlations within the analysis ensemble are not preserved, resulting in physical imbalances. Nevertheless, this behavior, which is analogous to the imbalances observed in standard local analysis schemes (e.g., [Hunt et al., 2007](#)), does not compromise the filter stability. Indeed, the physical balances are restored during the subsequent forecast step, where the model dynamics act as a smoother, re-establishing the cross-partition correlations before the next assimilation cycle.

The convergence of the proposed iterative VB algorithms to a local minimum of *theoretical* KLD is not guaranteed, notably owing to the underlying Gaussian and posterior independence assumptions on which these algorithms are founded (e.g. [Ait-El-Fquih et al., 2023](#); [Smidl and Quinn, 2006](#); [Sato, 2001](#); [Chappell et al., 2009](#); [Blei et al., 2017](#); [Ait-El-Fquih et al., 2020](#)). However, convergence towards a local minimum of the “*estimated*” KLD, i.e., approximated based on the ensembles, is guaranteed by construction (e.g. [Ait-El-Fquih et al., 2020](#)).

Characterizing the accuracy of VB-like approximations is not easy as this depends on several factors, including the number of partitions, K , and the strength of the posterior dependencies between these partitions (e.g. [Jordan et al., 1999](#); [Jaakkola and Jordan, 2000](#); [Jaakkola, 2001](#); [Smidl and Quinn, 2006](#)). Instead, one can intuitively examine the question of when the accuracy of VB approximation is likely to be reasonable and when one may expect it to fail. Clearly, when the state partitions are weakly (*a posteriori*) dependent, the VB estimate $\pi_n(\mathbf{x}_n) = \prod_{k=1}^K \pi_n(\mathbf{x}_n^k)$ of $p_n(\mathbf{x}_n)$ should be reasonable. In contrast, when these partitions become strongly dependent, the “assumption” of conditional independence becomes strong and this may jeopardize the VB estimation.

The VB estimation should (theoretically) improve with decreased number of partitions K , or equivalently with increased dimension d_p . However, in practice, since the pSEnKF and pETKF algorithms (without auxiliary localization) would be useful only when d_p does not exceed the ensemble size, M , the rule of thumb would be to choose, for a given M , a d_p that is as large as possible but not exceeding M .

The proposed pSEnKF and pETKF practically have similar algorithms as their respective standard counterparts, with the *Iterative Adjustment* as the sole extra component (see Algorithms 1 and 2). The Iterative Adjustment step has a computational cost that scales linearly with the state dimension, d_x , approximately equal to $\mathcal{C}_{\text{pSEnKF}}^{\text{extra}} = [2d_y + (6d_y + 2M)I] d_x$ flops⁶ in the pSEnKF and $\mathcal{C}_{\text{pETKF}}^{\text{extra}} = [2d_y + 6d_y I] d_x$ flops in the pETKF. The iterations’ number, I , is typically much smaller than d_x and d_y , a key property of the VB-type optimization algorithms (e.g., [Sato, 2001](#)). Thus, $\mathcal{C}_{\text{pSEnKF}}^{\text{extra}}$ and $\mathcal{C}_{\text{pETKF}}^{\text{extra}}$ should be insignificant in large-scale geophysical applications, compared to the costs of the SEnKF and ETKF analysis steps ($\sim \mathcal{O}(d_y^2 d_x)$ in linear observation models) and forecast step.

It is finally worth noting that the proposed iterative schemes are VB coordinate-descent procedures (specifically, cyclic coordinate ascent on the negative free energy) with analytical Kalman-like updates, rather than numerical linear solvers (e.g., Krylov subspace methods). Consequently, standard physical preconditioners are not directly applicable to these probabilistic updates. However, in high-dimensional or non-Gaussian scenarios, acceleration techniques may become useful, for instance, preconditioned Conjugate Gradient for solving large-scale innovation-covariance inversions, or natural-gradient methods ([Martens, 2020](#)) for optimization-based non-Gaussian updates.

⁶floating operations, see e.g., [Ait-El-Fquih and Hoteit \(2015\)](#).

5 Numerical experiments

Numerical experiments are conducted with the nonlinear Lorenz-96 (L96) model (Lorenz and Emanuel, 1998) to assess the behavior of the proposed pSEnKF and pETKF, and to evaluate their performances against the standard SEEnKF and ETKF using localization. L96 model simulates the time evolution of an atmospheric quantity based on differential equations:

$$\frac{dx(j, t)}{dt} = x(j-1, t)[x(j+1, t) - x(j-2, t)] - x(j, t) + F, \quad (40)$$

where $F = 8$ denotes the external forcing term, and $x(j, t)$, with $j = 1, \dots, d_x = 40$, the j -th element of the state at time t ; boundaries conditions are periodic (i.e., $x(-1, t) = x(d_x - 1, t)$, $x(0, t) = x(d_x, t)$, and $x(1, t) = x(d_x + 1, t)$).

The model (40) is numerically integrated using the fourth-order Runge-Kutta discretization scheme with a time step $\delta_m = 0.05$, equivalent to six hours in real time. The model is assumed perfect, and integrated forward to simulate a trajectory of 114600 time steps, starting from an initial state which elements (state variables) are set to F , except the 20-th one, which is set to $(1 + 0.001)F$. The first 100000 time steps of the resulting trajectory are discarded as a spin-up period, and the remaining 14600 time steps (i.e., 10 years in model time) are considered as the reference state trajectory, to be later estimated by the filters based on observations extracted from those reference states. The observations are extracted by adding to the states a Gaussian noise with zero mean and a covariance, $\mathbf{R} = r \times \mathbb{I}_{d_x}$, with $r = 0.6$, corresponding to a signal-to-noise-rate (SNR) of 15 dB, i.e.,

$$r = \frac{\sum_{n=0}^{T-1} \|\mathbf{H}_n \mathbf{x}_n\|^2}{T d_y} \times 10^{-\text{SNR}/10},$$

T being the total number of model time steps (e.g. Ait-El-Fquih and Hoteit, 2015).

We start by presenting the results of an experiment aiming at demonstrating the relevance of the proposed pSEnKF and pETKF with $M = 20$ members, in a full observational scenario (i.e., all state variables are observed) and a setting where the observations are assimilated every four model time steps (i.e., with an observations' time step, $\delta_o = 4 \delta_m$). In both filters, the initial forecast ensemble is generated from a Gaussian distribution centred around the mean of the model trajectory, and having $3\mathbb{I}_{d_x}$ as covariance. Their (iterative) analysis steps split the state into $K = 4$ partitions (of dimension $d_p = 10$), and assume convergence to be reached when the relative squared misfit norm of the full state analysis estimate, $\text{RSMN}^i = \|\hat{\mathbf{a}}_n^i - \hat{\mathbf{a}}_n^{i-1}\|^2 / \|\hat{\mathbf{a}}_n^{i-1}\|^2$, drops below 10^{-10} (this is equivalent to monitor convergence using NFE (44)-(45), as in the proposed filters only the analysis means vary over iterations whereas the covariances are kept fixed). Further both filters use inflation with a factor, of 1.1, chosen based on trial-and-error tuning.

To reduce statistical fluctuations, each experiment is repeated independently for 50 times, with different realizations of observational noises and initial ensembles. The average of the 50 runs is taken as the final result.

Fig. 1 displays the evolution over iterations of RSMN at assimilation cycles $n = 0, N/3, 2N/3$ and N , with N being the total number of assimilation cycles. As can be seen, both algorithms achieve convergence after 2 iterations only, consistent with the well-known fast convergence of VB-like filtering algorithms (e.g. Sato, 2001).

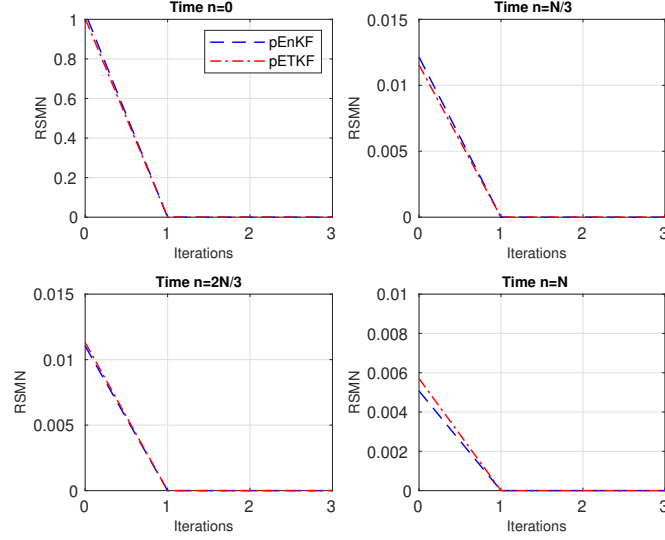


Figure 1: Evolution of the RSMN of the state analysis estimate as function of the iterations' number after every $N/3$ assimilation cycles, with N being their total number.

Fig. 2 plots the first four components of the reference state during the last 100 assimilation cycles (for better readability), and their analysis estimates as they result from the two proposed filters. As can be seen, the reference states are well tracked by both algorithms. The MSEs of the full state analysis estimates are further presented in Fig. 3, suggesting a slightly better accuracy for the (deterministic) pETKF, as it supports better small ensembles (here $M = 20$), compared to the (stochastic) pSEnKF.

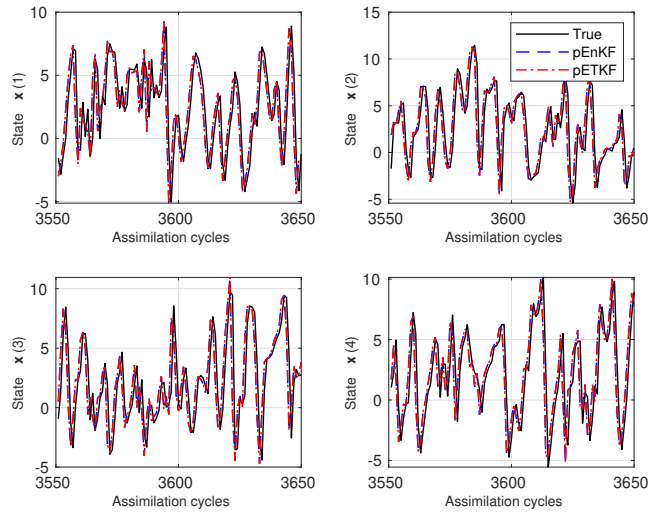


Figure 2: Tracking of the first 4 state variables with pSEnKF and pETKF within the last 100 assimilation cycles.

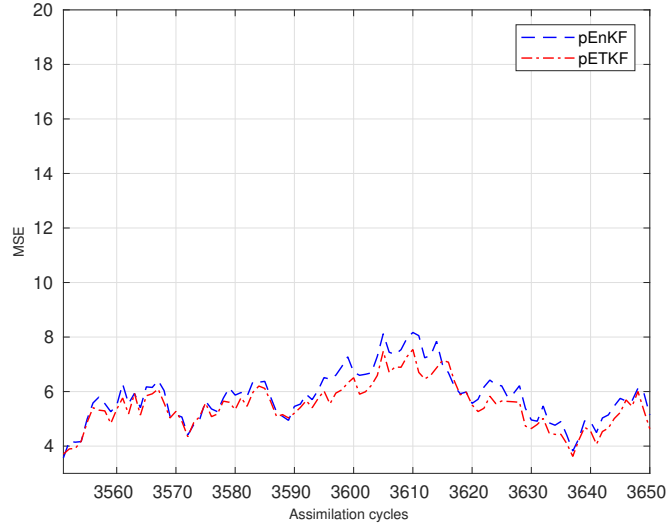


Figure 3: Time-evolution of the MSE of the analysis state estimate as provided by pSEnKF and pETKF within the last 100 assimilation cycles.

The second set of experiments is intended to assess the behavior of the proposed filters and to evaluate their performances against SEEnKF and ETKF using empirically tuned inflation and localization, in two different observational scenarios: full (i.e., all state variables are observed), and spatially sparse, assimilating half (i.e., odd-indexed variables are observed) and quarter (i.e., every fourth variable is observed) of the state variables. SEEnKF uses a covariance localization based on the fifth-order correlation function given in Gaspari and Cohn (1999) (Hamill et al., 2001), and ETKF uses the local analysis approach (Houtekamer and Mitchell, 1998). In each scenario, a series of sensitivity experiments is performed with different levels of noise in the data (SNR = 10, 15 dB, respectively corresponding to $r = 1.87, 0.6$) and different ensemble sizes ($M = 10, 20, 30$). The root MSE (RMSE) misfit between the reference states and their analysis estimates, averaged over the whole assimilation period, is used to evaluate the performances of the filters.

5.1 Full observational scenario

The averaged analysis RMSEs resulting from the four filters when observations of all model variables are assimilated are presented in Fig. 4. Panels (a) and (b) represent the cases of SNR = 15 dB and 10 dB, respectively, and Panel (c) the corresponding ratios, i.e., the ratios of the RMSEs obtained for SNR = 10 dB w.r.t. those associated to the case SNR = 15 dB. The RMSEs of the pSEnKF and pETKF in Fig. 4 (ditto for Figs. 5, 6 and 8 below) are obtained after trial-and-error tests using different values of partitions' size, i.e., $d_p = 1, 2, 5$ for $M = 10$, $d_p = 1, 2, 5, 10$ for $M = 20$, and $d_p = 1, 2, 5, 10, 20$ for $M = 30$. The “best” values of d_p here, i.e., those that correspond to the RMSEs in Fig. 4, are reported in Table 1.

As can be seen from Table 1, the d_p values that achieve the lowest RMSEs increase with the ensemble size, M . Following the discussion in Section 4.3, this is due to the back-to-back approximation (VB density approximation, which improves with increased d_p , combined with ensemble approximation, which improves with increased M) on which these filters are based. This combination suggests that obtaining the lowest RMSE when increasing M is conditioned by an increase of d_p , subject to d_p remaining smaller than M (in order to avoid the need of localization). On the other hand, Table 1 also suggests that, for a fixed M , the lowest RMSE can be achieved when the state partition corresponds to either the largest d_p value (among the tested ones) or to the one that precedes it. Taking for instance pSEnKF and SNR = 10 dB:

with $M = 20$ members the lowest RMSE is achieved when $d_p = 10$ (the largest value among the tested ones: $\{1, 2, 5, 10\}$), and with $M = 30$ it is achieved when $d_p = 10$ (the second largest value among those tested: $\{1, 2, 5, 10, 20\}$). Yet, it is important to note that increasing the ensemble can lead to better results for $d_p = 20$ compared to 10. In this regard, additional experiments with a larger ensemble ($M = 40$) have led to RMSE = 0.61628 for $d_p = 10$ and 0.60297 for $d_p = 20$.

The RMSEs reported in Fig. 4 suggest that, as expected, all the filters behave better with large ensembles and less noisy observations. The filters further overall exhibit comparable performances, providing RMSEs that are more or less close to each other, as will be further discussed below.

As Panels (a) and (b) show, when a small ensemble is used (i.e., $M = 10$ members), the deterministic ETKF and pETKF filters outperform their stochastic counterparts, regardless of the level of the noise in the observations (Hoteit et al., 2015). Such a difference becomes less significant with larger ensembles.

As Panel (c) shows, all the filters exhibit approximately twice larger errors when passing from assimilated observations with SNR = 15 dB to those with SNR = 10 dB.

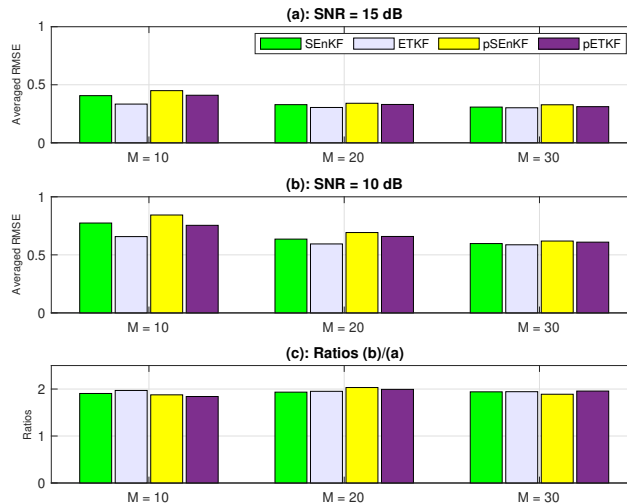


Figure 4: Averaged RMSEs of the state analysis estimates as provided by SEnKF, ETKF, pSEnKF and pETKF applied, with different ensemble sizes, on observations of SNR = 15 dB (Panel (a)) and 10 dB (Panel (b)). Panel (c) reports the ratios of RMSEs in Panel (b) w.r.t. those in Panel (a).

Table 1: The values of d_p that correspond to the errors plotted in Fig. 4.

	SNR = 15 dB			SNR = 10 dB		
	$M = 10$	$M = 20$	$M = 30$	$M = 10$	$M = 20$	$M = 30$
pSEnKF	5	10	20	5	10	10
pETKF	5	10	20	5	10	20

5.2 Spatially sparse observational scenario

We start by the scenario where half of the observations are assimilated and plot the resulting averaged analysis REMSs in Fig. 5. The partitions' sizes, d_p , that correspond to these (minimum) errors following trial-and-error tests are reported in Table 2.

The results in Table 2 are close to those in Table 1. Notably, the values of d_p that achieve the lowest RMSEs increase with the ensemble size, M , and for each M , the state partitioning that provides the lowest RMSE corresponds to one of the two largest values of d_p among the tested ones.

The RMSEs in Fig. 5 are found to be larger than those in Fig. 4, which is expected as less observations are assimilated in this experiment. They further generally decrease with the ensemble size and less noisy observations.

Fig. 5 also shows that the four filters overall exhibit comparable performances, providing RMSEs that are more or less close to each other. Specifically, when $M = 10$ members are used, the proposed pSEnKF and pETKF slightly underperform their standard counterparts (most notably when SNR = 10 dB). Such a behavior becomes less significant with larger ensembles ($M = 20$ and 30 members).

Overall, similar results are obtained in the quarter observational scenario, as can be noticed from Fig. 6 and Table 3, yet with the exception of the RMSEs being less sensitive to more noise in the observations.

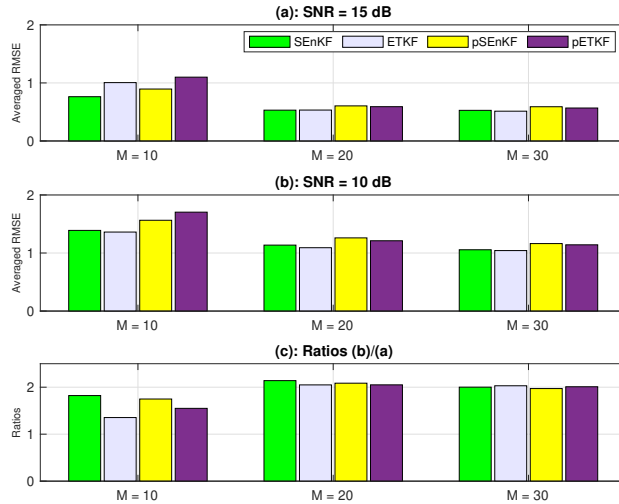


Figure 5: As in Fig. 4, but with observing odd-indexed state variables only.

Table 2: The values of d_p that correspond to the errors plotted in Fig. 5.

	SNR = 15 dB			SNR = 10 dB		
	$M = 10$	$M = 20$	$M = 30$	$M = 10$	$M = 20$	$M = 30$
pSEnKF	5	10	10	5	10	10
pETKF	2	5	20	2	10	20

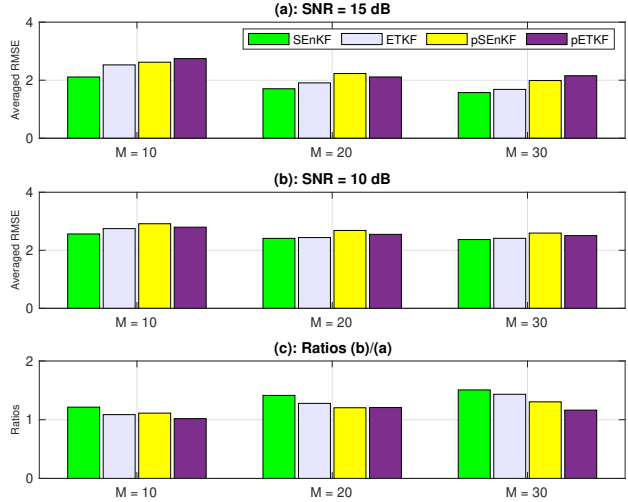


Figure 6: As in Fig. 4, but with observing every fourth state variable.

Table 3: The values of d_p that correspond to the errors plotted in Fig. 6.

	SNR = 15 dB			SNR = 10 dB		
	$M = 10$	$M = 20$	$M = 30$	$M = 10$	$M = 20$	$M = 30$
pSEnKF	5	10	10	5	5	10
pETKF	2	5	10	5	5	10

We further assess the statistical consistency of the proposed partitioned approach by comparing the analysis ensemble spread against the (time-series) analysis RMSE. For that, we use pSEnKF with $d_p = 10$ (i.e., four partitions) and $M = 30$ in the configuration “SNR = 15 dB, half observational scenario” (Panel (a) in Fig. 5). The goal is to determine whether the partition-wise update results in under- or over-dispersive ensembles and to identify potential artifacts/imbalances in uncertainty near the partition boundaries. To achieve this, we categorize the state indices/elements into four subsets based on their observational status (observed vs. unobserved) and their proximity to partition boundaries. Components are considered as “Close” if they lie within two grid points of a boundary, while the remaining (interior) components are classified as “Far”.

Such four subsets correspond to: {Observed and Close}, {Unobserved and Close}, {Observed and Far}, and {Unobserved and Far}. For each assimilation cycle, the analysis ensemble spread and RMSE are computed independently using pSEnKF across these subsets.

The results are reported in Fig. 7. As expected, unobserved variables (Panels b and d) exhibit larger errors and spread compared to observed ones (Panels a and c). The ensemble spread further demonstrates a clear consistency with the RMSE as it closely tracks it in all subsets. In particular, the filter does not suffer from under-dispersion at the partition boundaries (Panels a and b), even for unobserved variables. In other terms, the partitioning did not induce noticeable boundary artifacts in the spread and error. This suggests that the iterative adjustment in the analysis step, combined with the mixing provided by the model dynamics in the forecast step, effectively propagates information across partitions and preserves a coherent ensemble spread globally, avoiding artificial discontinuities at the boundaries of the partitions.

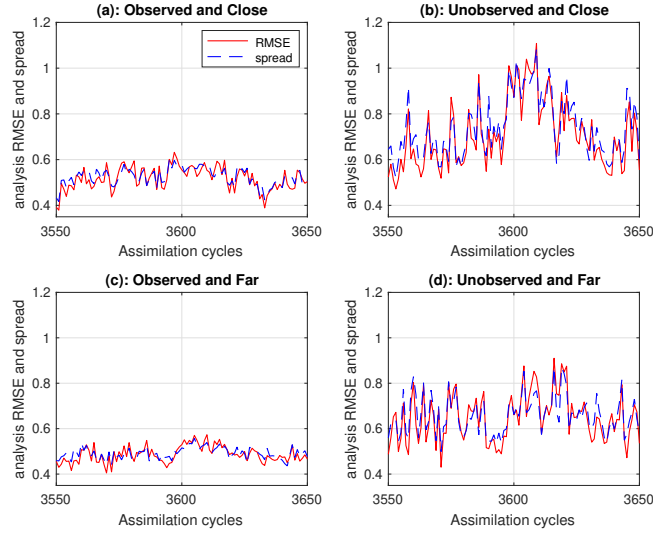


Figure 7: Time-evolution of the analysis RMSE and ensemble spread as provided, within the last 100 assimilation cycles, by pSEnKF implemented with $M = 30$ members and $d_p = 10$ in the half observational scenario with SNR = 15 dB (one scenario of Panel (a) in Fig. 5). The results are averaged independently over four subsets of state variables defined based on their observability and proximity to partition boundaries.

5.3 More challenging scenarios

The case of SNR = 10 dB, $M = 10$ and $\delta_o = 4\delta_m$ in the quarter observational scenario (i.e., Fig. 6) is the most challenging among those presented so far (this case will hereafter refer to Case 0). Here, we examine the robustness of the filters to even more challenging case scenarios favouring additional systematic errors, through increasing the observations' temporal sparsity and using wrong models in the filtering algorithms. These include four case scenarios, sorted below according to their complexity:

- Case 1: Case 0, with $\delta_o = 8\delta_m$ instead of $4\delta_m$;
- Case 2: Case 1, with a bias of $0.3F$ induced in the state model during the filtering;
- Case 3: Case 2, with a bias of $0.3\mathbf{H}\mathbf{x}_0$ induced in the observation model during the filtering;
- Case 4: Case 3, with reducing the (true) observation noise covariance \mathbf{R} by 30% during the filtering (i.e., $0.7\mathbf{R}$ is used as the prescribed observation noise covariance in assimilation, while \mathbf{R} is the true observation noise covariance used in generating observations from truth).

Fig. 8 plots the resulted averaged analysis RMSEs. As can be seen from comparing Case 1 with Case 0, all the filters are clearly sensitive to less frequent observations. In Case 1, the proposed filters still underperform the standard SEEnKF, in a similar way to Case 0 although less significantly. Compared to ETKF, the pSEnKF is however found to achieve a very closer behavior and the pETKF became even slightly more accurate.

Comparing Case 2 with Case 1, it turns out that the effect of a bias in the state model is slightly more pronounced on the standard filters than on the proposed ones. This may reflect a slightly more deterioration of the forecast background in the standard filters, caused by the use of the erroneous model. One further notes that in Case 2, the pSEnKF and pETKF behaviors became closer to that of SEEnKF, and clearly better than that of ETKF.

All the filters are found to be significantly affected where a bias is induced in the observation model too (Case 3), exhibiting RMSEs that significantly increase when moving from Case 2 to Case 3. In Case 3, the two proposed filters are further found to significantly outperform the ETKF and slightly the SEnKF.

As can be seen from Cases 3 and 4, the proposed pSEnKF and pETKF filters, and to a slightly lesser extent the standard filters, seem to be robust to increased confidence in wrong observations (the effect of deflating \mathbf{R} by 30% is more or less insignificant). Furthermore, the gap between the RMSEs of the standard filters and those of the proposed ones has been found to increase when moving from Case 3 to Case 4. The outperformance of the proposed filters in such challenging scenarios likely stems from their design: they use the same observational information as the standard filters but apply it to smaller state partitions, updated iteratively. This localized and iterative update scheme reduces the impact of parameter errors and enhances stability under challenging conditions.

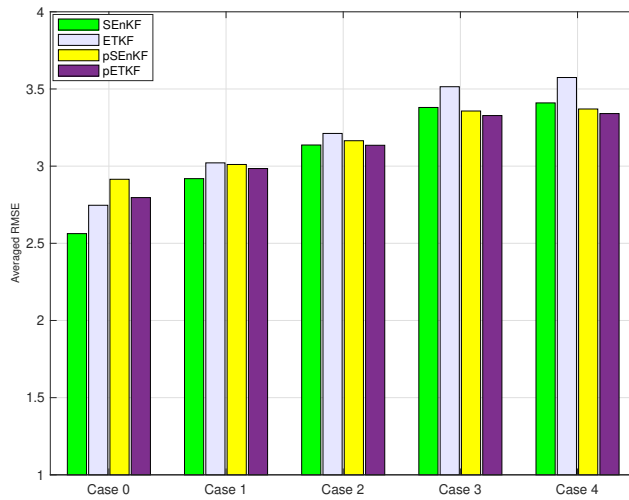


Figure 8: Averaged RMSEs of the state analysis estimates as provided by SEnKF, ETKF, pSEnKF and pETKF in different challenging case scenarios.

It is further worth assessing the relevance of the assimilation through comparisons against baselines, such as the climatological level of variability, σ_{clim} , which gives an idea on how large the natural fluctuations of the truth (nature run) are, and the time-series RMSE of the observations, rmse_{obs} . These are respectively defined as,

$$\sigma_{\text{clim}} = \frac{1}{\sqrt{d_x}} \|\boldsymbol{\delta}\|,$$

$$\text{rmse}_{\text{obs}}(n) = \frac{1}{\sqrt{T}} \|\mathbf{y}_n - \mathbf{H}_n \mathbf{x}_n\|,$$

where the i -th element of the $(d_x \times 1)$ sized vector $\boldsymbol{\delta}$ is defined as $\delta^i = \sqrt{\frac{1}{T} \sum_{n=0}^{T-1} (x_n^i - \bar{x}^i)^2}$, \mathbf{x}_n and \mathbf{y}_n respectively denote the reference state and the observation at assimilation time n , and \bar{x}^i the (temporal) average of $\{x_n^i\}_n$.

Fig. 9 plots these quantities and the temporal rmse errors of the state analysis estimates provided by the four filters in Cases 0 and 4, within the last 100 assimilation cycles. According to the results in Panel (a), although the filters, including the standard ones, seem to not fit the data very well in such a challenging scenario (as their analysis rmse errors exceed rmse_{obs}), they remain clearly useful relatively to the climatological mean (as their analysis rmse errors

are clearly smaller than σ_{clim}). In Panel (a), one also recognizes the order of the analysis errors indicated in Fig. 8, i.e., overall SEnKF outperforms ETKF, then pETKF and pSEnKF.

When the filters further run with larger assimilation cycles and perturbed parameters (Panel (b)), the analysis errors increase, compared to those in Panel (a), but overall remain below σ_{clim} , suggesting that the assimilation results remain meaningful even in a such challenging scenario.

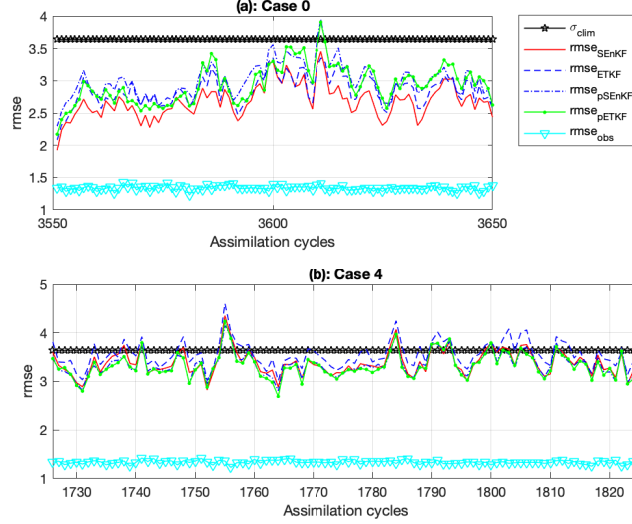


Figure 9: The climatological level of variability and the time-series rmse of the observations and the state analysis estimates provided by the four filters in Cases 0 and 4, within the last 100 assimilation cycles.

5.4 A case of non-uniform state partitioning

As previously outlined, the proposed schemes are straightforward to adapt to the case where the K partitions \mathbf{x}_n^k have different sizes d_{p^k} , by only replacing in Algorithms 1 and 2 d_p by d_{p^k} and Kd_p by $\sum_{k=1}^K d_{p^k}$. Two configurations are considered here:

- *Configuration 1:* The state is split into $K = 3$ partitions of dimensions $[d_{p^1}, d_{p^2}, d_{p^3}]$ that can be equal to $\mathcal{D}_3^1 = [15, 13, 12]$, $\mathcal{D}_3^2 = [17, 11, 12]$, $\mathcal{D}_3^3 = [16, 15, 9]$ or $\mathcal{D}_3^4 = [10, 20, 10]$.
- *Configuration 2:* The state is split into $K = 4$ partitions of dimensions $[d_{p^1}, d_{p^2}, d_{p^3}, d_{p^4}]$ that can be equal to $\mathcal{D}_4^1 = [9, 2, 15, 14]$, $\mathcal{D}_4^2 = [6, 15, 9, 10]$, $\mathcal{D}_4^3 = [10, 10, 10, 10]$ or $\mathcal{D}_4^4 = [10, 8, 13, 9]$.

For each case, the proposed filters are run using $M = 30$ members in a non-uniform half observational scenario, in which the variables $\{y_n^i; i = 1, 4, 5, 8, 10, 12, 13, 14, 17, 20, 24, 25, 27, 28, 31, 32, 34, 35, 37, 40\}$ are observed, $\text{SNR} = 15$ dB and $\delta_o = 4\delta_m$. The standard filters are also run with “optimally” tuned inflation and localization.

Fig. 10 plots the percentage of the difference between the averaged state analysis RMSEs as resulting from the proposed filters and those obtained by the standard filters, defined as,

$$\frac{\text{RMSE}_{\text{proposed filter}} - \text{RMSE}_{\text{standard filter}}}{\text{RMSE}_{\text{standard filter}}} \times 100.$$

Overall, the proposed filters in both configurations provide close performances to the standard ones.

As can be seen from Panel (a), with all three-part state partitions, the pETKF achieved RMSEs that do not exceed 5.2% of the RMSEs provided by both standard filters. It even

behaved as good as ETKF when it is implemented with \mathcal{D}_3^1 or \mathcal{D}_3^2 . The pSEnKF performs less than pETKF, achieving its best performance when implemented with \mathcal{D}_3^1 or \mathcal{D}_3^2 , cases in which it has suggested RMSEs that are respectively 3.79% and 3.9% larger than that of ETKF.

In the four-part partitioning configuration (Panel (b)), the percentage errors do not exceed 10%, like in Panel (a), but are overall larger than those in Panel (a). This suggests that in this observational scenario, it is generally more beneficial to split the state into three partitions instead of four.

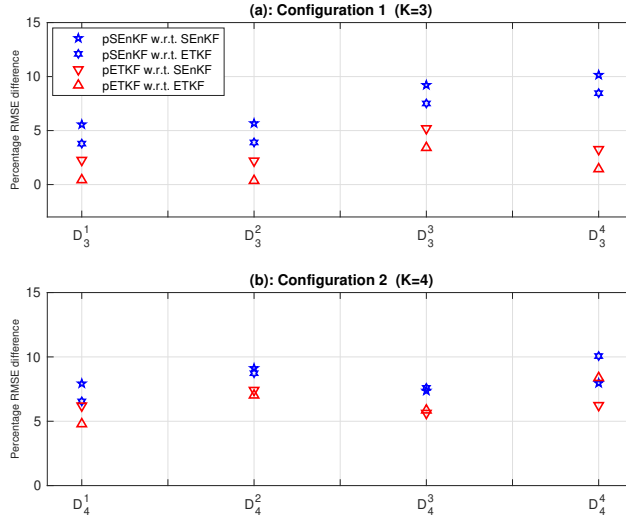


Figure 10: The difference (in %) between the averaged state analysis RMSEs provided by the standard SEEnKF and ETKF and those provided by the proposed pSEnKF and pETKF splitting the state non-uniformly following Configurations 1 (Panel (a)) and 2 (Panel (b)), all using $M = 30$ members in a non-uniform half observational scenario with SNR = 15 dB and $\delta_o = 4\delta_m$.

5.5 Illustration through assimilating a single observation

To illustrate how the proposed approach deals with (sampling and systematic) noises, single observation experiments are conducted, observing only the 20th state variable with SNR = 15 dB. Fig. 11 plots the time evolution of the analysis increment (the analysis mean minus the forecast mean) over the last 100 assimilation cycles as provided by pSEnKF using $M = 30$ members, $\delta_o = 4\delta_m$ and splitting the state vector into partitions of size $d_p = 8$ (pETKF have led to similar results, but they are not included here to limit the length of the paper). As can be seen from Fig. 11, the analysis increments are localized around the position of the observation, meaning that the localization works as expected.

Fig. 11 also shows that during the analysis cycle, the information from the observation has been retained within the state partition in which it is located (i.e., the partition $\mathbf{x}_n^3 = (x_n^{17}, \dots, x_n^{24})$), and did not propagate across the other partitions. This is due to i) the removal of the forecast cross-covariances (i.e., to $\mathbf{G}_n^k = \mathbf{0}$), combined with ii) the particular structure of \mathbf{H} ($= [0, \dots, 0, 1, 0, \dots, 0]$) which arises in this single-observation case. Indeed, since $\mathbf{G}_n^k = \mathbf{0}$, the update of the state partitions is performed by the analysis Eq. (31) instead of Eq. (27), and due to the sparse structure of \mathbf{H} , the Kalman gains \mathbf{L}_n^k in Eq. (31) that are associated to all partitions, except the one that contains the observation (i.e., \mathbf{x}_n^3), become null. This results in analysis estimates that are identical to the forecast estimates (i.e., with no analysis increments) in the partitions that do not include the observation.

For a similar reason, the standard SEEnKF with tuned covariance localization (with an “optimal” length-scale $\ell_s = 2$) has been found to exhibit a similar behavior (cf. Fig. 12). More pre-

cisely, the relatively strong localization ($\ell_s = 2$) drastically limits the forecast cross-covariances, and this, together with the particular structure of \mathbf{H} , limits the propagation of the information in the observation only within the close neighborhood. In that respect, these two filters lead to comparable RMSEs: 3.6315 for pSEnKF and 3.6245 for SEEnKF.

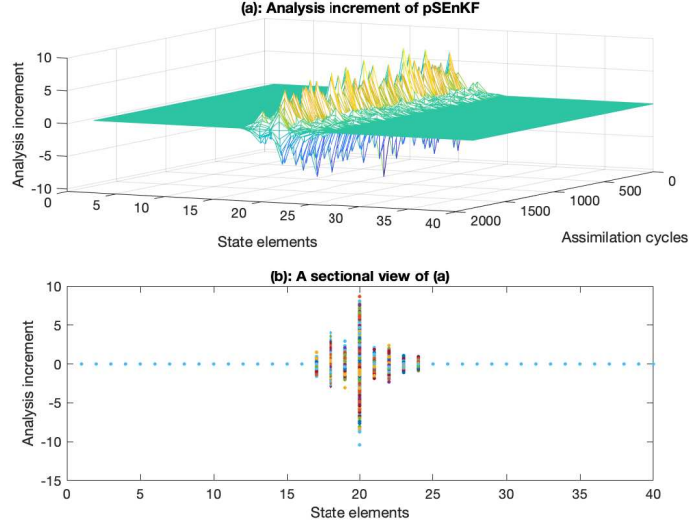


Figure 11: a) Time-evolution of the analysis increment of all state elements as provided, within the last 100 assimilation cycles, by pSEnKF implemented with $M = 30$ members, $d_p = 8$ and “optimal” inflation (with factor $\alpha = 1.1$). (b) is a sectional view of (a). Only the 20th state element is observed and assimilated.

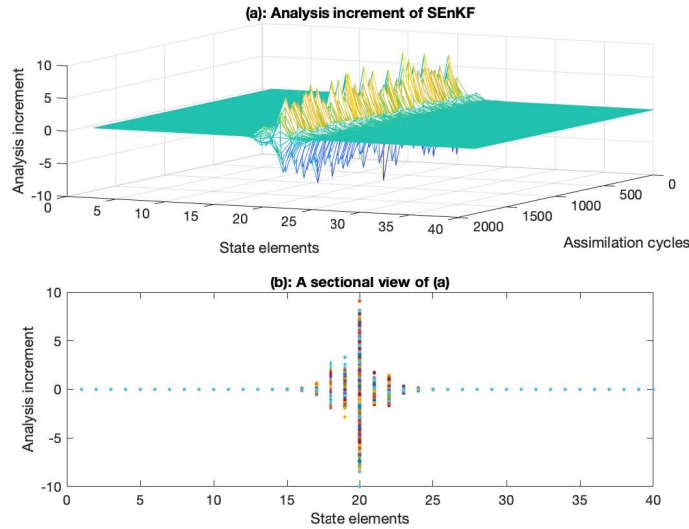


Figure 12: a) Time-evolution of the analysis increment of all state elements as provided, within the last 100 assimilation cycles, by SEEnKF implemented with $M = 30$ members, “optimal” inflation (with factor $\alpha = 1.1$) and localization (with length-scale $\ell_s = 2$). (b) is a sectional view of (a). Only the 20th state element is observed and assimilated.

Finally, to investigate the effect of larger partition size in this single-observation scenario, we repeated the experiment of Fig. 11 with $d_p = 20$ instead of 8. Results not shown here indicate that the increment remains confined to the partition containing the observed component (no

cross-partition long-range effects), while the within-partition spatial extent naturally broadens. RMSE slightly degrades compared with the $d_p = 8$ case (Fig. 11), but improves when M is increased (RMSE = 3.6383 and 3.6287 respectively for $M = 40$ and 45), consistent with sampling limitations when d_p becomes large relative to M .

Overall, this confirms that larger partitions are most beneficial when supported by a sufficiently large ensemble, and suggests that d_p effectively controls a discrete (partition-wise) localization scale, subject to the usual ensemble-size sampling constraint: reliable within-partition covariance estimation requires M to be sufficiently large relative to d_p (in practice $M > d_p$, and ideally $M \gg d_p$).

6 Conclusion

This work proposes an ensemble Kalman filtering (EnKF) approach that is inherently localized, avoiding the need for any auxiliary localization technique. Its principle is based on first localizing the continuous analysis probability density function (pdf), then applying Gaussian-like ensemble Kalman sampling procedures on the localized pdf. The localization of the analysis pdf consists of approximating it by a product of independent marginal pdfs corresponding to small partitions of the state vector, using the variational Bayesian optimization. These marginals are then sampled following stochastic EnKF (SEnKF) and deterministic ensemble transform Kalman filtering (ETKF) procedures, but any other sampling procedure could be applied too. The rationale behind the proposed approach relies on the assumption that selecting partitions with dimensions smaller than the ensemble size should boost performances without incorporating any external localization scheme, while mitigating for the effect of undersampling and systematic errors.

Algorithmically speaking, the filters involve the same forecast step as the standard SEnKF and ETKF, but different analysis steps which consist in iteratively adjusting the standard SEnKF and ETKF updates of each partition, with a shift by a linear combination of the ensemble means of the other partitions. Numerical experiments are conducted with the Lorenz-96 model under various challenging settings and scenarios, demonstrating the relevance of the proposed filters in geophysical applications, being generally comparable to the SEnKF and ETKF with already tuned localization (and sometimes even better than them), both in terms of computational burden and estimation accuracy.

Future work will consider enhancing the new filters' performances by integrating computationally reasonable approximations of the gain terms in Eqs. (24)-(25), and by mitigating for the imposed posterior independencies between the state partitions following e.g. the approach of (Ranganath et al., 2016). We will also consider integrating the online estimation of the inflation factor as e.g. in (Ait-El-Fquih and Hoteit, 2020), with the goal to derive more autonomous ensemble filtering schemes, avoiding the need for trial-and-error tuning of this factor. Other important directions for future work would be to apply the proposed inherently localized approach on other deterministic ensemble filters, e.g., SEIK (Hoteit et al., 2002), LETKF (Hunt et al., 2007), and to apply all the new filters to realistic oceanic and atmospheric data assimilation problems.

Appendix

The analysis step of the generic localized filter

We show how (22)-(28) can be derived from (21).

The Gaussian expression (3) of $p(\mathbf{y}_n|\mathbf{x}_n)$ entails,

$$p(\mathbf{y}_n|\mathbf{x}_n) \propto \exp\left(-\frac{1}{2}\|\mathbf{y}_n - \mathbf{H}_n^k \mathbf{x}_n^k - \mathbf{H}_n^k \mathbf{x}_n^k\|_{\mathbf{R}_n}^2\right). \quad (41)$$

Applying the ln function to (41), followed by the expectation w.r.t. $\pi_n^{(i,i-1)}(\mathbf{x}_n^{k-}) = \prod_{j=1}^{k-1} \pi_n^i(\mathbf{x}_n^j) \times \prod_{j=k+1}^K \pi_n^{i-1}(\mathbf{x}_n^j)$, then the exp function, one obtains,

$$\begin{aligned} \mathcal{L}_{\mathbf{y}_n}^i(\mathbf{x}_n^k) &\propto \exp\left(\mathbb{E}_{\pi_n^{(i,i-1)}(\mathbf{x}_n^{k-})}[\ln p(\mathbf{y}_n|\mathbf{x}_n)]\right), \\ &\propto \exp\left(-\frac{1}{2}\|\mathbf{y}_n - \mathbf{H}_n^{k-}\hat{\mathbf{m}}_{n|n}^{k-,i} - \mathbf{H}_n^k\mathbf{x}_n^k\|_{\mathbf{R}_n^{-1}}^2\right), \\ &= (22). \end{aligned}$$

We now derive $\pi_{n-1}^i(\mathbf{x}_n^k)$ (23)-(25). One first shows that,

$$\begin{aligned} \pi_{n-1}^i(\mathbf{x}_n^k) &\propto \exp\left(\mathbb{E}_{\pi_n^{(i,i-1)}(\mathbf{x}_n^{k-})}[\ln p_{n-1}(\mathbf{x}_n)]\right), \\ &\propto \exp\left(\mathbb{E}_{\pi_n^{(i,i-1)}(\mathbf{x}_n^{k-})}[\ln p(\mathbf{x}_n^k|\mathbf{x}_n^{k-}, \mathcal{Y}_{n-1})]\right). \end{aligned} \quad (42)$$

On the other hand, the Gaussian assumption on $p_{n-1}(\mathbf{x}_n)$ (i.e., $\mathcal{N}_{\mathbf{x}_n}(\hat{\mathbf{x}}_{n|n-1}, \mathbf{P}_{n|n-1})$) implies that the conditional distribution $p(\mathbf{x}_n^k|\mathbf{x}_n^{k-}, \mathcal{Y}_{n-1})$ is also Gaussian with mean $\boldsymbol{\mu}_n(\mathbf{x}_n^{k-}) = \hat{\mathbf{x}}_{n|n-1}^k + \mathbf{G}_n^k(\mathbf{x}_n^{k-} - \hat{\mathbf{x}}_{n|n-1}^{k-})$, and covariance $\boldsymbol{\Sigma}_n = \mathbf{P}_{n|n-1}^k - \mathbf{G}_n^k\mathbf{P}_{n|n-1}^{k-,k}$, where $\mathbf{G}_n^k = \mathbf{P}_{n|n-1}^{k,k}(\mathbf{P}_{n|n-1}^{k-})^{-1}$, and $\mathbf{P}_{n|n-1}^k$, $\mathbf{P}_{n|n-1}^{k-}$, $\mathbf{P}_{n|n-1}^{k-,k}$ and $\mathbf{P}_{n|n-1}^{k-,k}$ are extracted from $\mathbf{P}_{n|n-1}$ according to the positions k and k^- (e.g., Ait-El-Fquih and Desbouvries, 2011, Appendix, Prop. 9). In an ensemble setting, the supposedly large $(d_x - d_p) \times (d_x - d_p)$ -sized covariances $\mathbf{P}_{n|n-1}^{k-}$ are approximated based on a small number M of forecast members, meaning that these are singular, thus non-invertible. In such a case, the inverse $(\mathbf{P}_{n|n-1}^{k-})^{-1}$ in the expression of \mathbf{G}_n^k is replaced by a pseudo-inverse, $(\mathbf{P}_{n|n-1}^{k-})^+$ (e.g., Anderson and Moore, 1979, Sec. 2.3).

Now, following a similar derivation to that of $\mathcal{L}_{\mathbf{y}_n}^i(\mathbf{x}_n^k)$ above, we apply the ln function to $p(\mathbf{x}_n^k|\mathbf{x}_n^{k-}, \mathcal{Y}_{n-1}) = \mathcal{N}_{\mathbf{x}_n^k}(\boldsymbol{\mu}_n, \boldsymbol{\Sigma}_n)$, followed by the expectation w.r.t. $\pi_n^{(i,i-1)}(\mathbf{x}_n^{k-})$, then the exp function, to readily obtain (23)-(25).

One still has to derive $\pi_n^i(\mathbf{x}_n^k)$ (26)-(28). Since the VB pdf of \mathbf{x}_n^k , $\pi_{n-1}^i(\mathbf{x}_n^k)$ (23), is Gaussian, and the VB pdf of \mathbf{y}_n conditioned on \mathbf{x}_n^k , $\mathcal{L}_{\mathbf{y}_n}^i(\mathbf{x}_n^k)$ (22), is Gaussian with a mean linear in \mathbf{x}_n^k , then the associated joint pdf, $\kappa^i(\mathbf{x}_n^k, \mathbf{y}_n) = \pi_{n-1}^i(\mathbf{x}_n^k)\mathcal{L}_{\mathbf{y}_n}^i(\mathbf{x}_n^k)$, is Gaussian with parameters given as (e.g., Ait-El-Fquih and Desbouvries, 2011, Appendix, Prop. 8),

$$\kappa^i(\mathbf{x}_n^k, \mathbf{y}_n) = \mathcal{N}_{(\mathbf{x}_n^k, \mathbf{y}_n)}\left(\begin{bmatrix} \mathbf{m}_{n|n-1}^{k,i} \\ \mathbf{H}_n^k\mathbf{m}_{n|n-1}^{k,i} + \mathbf{H}_n^{k-}\mathbf{m}_{n|n}^{k-,i} \end{bmatrix}, \begin{bmatrix} \mathbf{C}_{n|n-1}^k & \mathbf{C}_{n|n-1}^k(\mathbf{H}_n^k)^T \\ \mathbf{H}_n^k\mathbf{C}_{n|n-1}^k & \mathbf{H}_n^k\mathbf{C}_{n|n-1}^k(\mathbf{H}_n^k)^T + \mathbf{R}_n \end{bmatrix}\right) \quad (43)$$

The VB pdf of interest, $\pi_n^i(\mathbf{x}_n^k) = \kappa^i(\mathbf{x}_n^k|\mathbf{y}_n)$, is then obtained from a conditioning of Eq. (43) using Prop. 9 of (Ait-El-Fquih and Desbouvries, 2011, Appendix). By doing so, one immediately obtains (26)-(28).

The practical computation of NFE over iterations

From Eq. (13), the NFE at assimilation time t_n and iteration i is defined as,

$$\begin{aligned} \text{NFE}^i &= \mathbb{E}_{\pi_n^i(\mathbf{x}_n)}[\ln p(\mathbf{x}_n, \mathbf{y}_n|\mathcal{Y}_{n-1})] - \overbrace{\mathbb{E}_{\pi_n^i(\mathbf{x}_n)}[\ln \pi_n^i(\mathbf{x}_n)]}^{\phi_3^i} \\ &= \underbrace{\mathbb{E}_{\pi_n^i(\mathbf{x}_n)}[\ln p(\mathbf{y}_n|\mathbf{x}_n)]}_{\phi_1^i} + \underbrace{\mathbb{E}_{\pi_n^i(\mathbf{x}_n)}[\ln p_{n-1}(\mathbf{x}_n)]}_{\phi_2^i} - \phi_3^i. \end{aligned} \quad (44)$$

Inserting in the above ϕ^i terms the Gaussians $p(\mathbf{y}_n|\mathbf{x}_n) = \mathcal{N}_{\mathbf{y}_n}(\mathbf{H}_n\mathbf{x}_n, \mathbf{R}_n)$, $p_{n-1}(\mathbf{x}_n) \approx \mathcal{N}_{\mathbf{x}_n}(\hat{\mathbf{f}}_n, \mathbf{P}_{\mathbf{f}_n})$ and $\pi_n^i(\mathbf{x}_n) \approx \mathcal{N}_{\mathbf{x}_n}(\hat{\mathbf{a}}_n^i, \mathbf{P}_{\mathbf{a}_n})$, with $\mathbf{P}_{\mathbf{f}_n}$ and $\mathbf{P}_{\mathbf{a}_n}$ are block-diagonal covariances formed based on

the ensemble perturbation matrices $\{\mathbf{S}_{\mathbf{f}_n^k}\}_k$ and $\{\mathbf{S}_{\mathbf{a}_n^k}\}_k$, one obtains,

$$\begin{cases} \phi_1^i \approx -\frac{1}{2} \left[\ln((2\pi)^{d_y} |\mathbf{R}_n|) + \text{Tr}(\mathbf{P}_{\mathbf{a}_n} \mathbf{H}_n^T \mathbf{R}_n^{-1} \mathbf{H}_n) + \|\mathbf{y}_n - \mathbf{H}_n \hat{\mathbf{a}}_n^i\|_{\mathbf{R}_n^{-1}}^2 \right], \\ \phi_2^i \approx -\frac{1}{2} \left[\ln((2\pi)^{d_x} |\mathbf{P}_{\mathbf{f}_n}|) + \text{Tr}(\mathbf{P}_{\mathbf{a}_n} \mathbf{P}_{\mathbf{f}_n}^{-1}) + \|\hat{\mathbf{a}}_n^i - \hat{\mathbf{f}}_n\|_{\mathbf{P}_{\mathbf{f}_n}^{-1}}^2 \right], \\ \phi_3^i \approx -\frac{1}{2} [\ln((2\pi)^{d_x} |\mathbf{P}_{\mathbf{a}_n}|) + d_x]. \end{cases} \quad (45)$$

Eqs. (45) are then inserted in Eq. (44) to obtain an ensemble-based approximate expression of NFEⁱ.

Acknowledgments

The authors thank the anonymous reviewers for the valuable and constructive comments.

Data Availability Statement

Data sharing not applicable – no new data generated.

Author Contributions

Boujemaa Ait-El-Fquih: conceptualization; investigation; writing - original draft; methodology; writing - review & editing.

Ibrahim Hoteit: conceptualization; funding acquisition; resources; writing - review & editing.

ORCID

Boujemaa Ait-El-Fquih  <https://orcid.org/0000-0003-1119-7585>

Ibrahim Hoteit  <https://orcid.org/0000-0002-3751-4393>

References

- M. Ades and P. van Leeuwen. An exploration of the equivalent weights particle filter. *Quarterly Journal of the Royal Meteorological Society*, 139:820–40, 2013.
- B. Ait-El-Fquih and F. Desbouvries. Kalman filtering in triplet Markov chains. *IEEE Transactions on Signal Processing*, 54(8):2957–63, Aug. 2006.
- B. Ait-El-Fquih and F. Desbouvries. Fixed-Interval Kalman Smoothing Algorithms in singular state-space systems. *The Journal of Signal Processing Systems*, 65(3):469–78, December 2011.
- B. Ait-El-Fquih and I. Hoteit. Fast Kalman-like Filtering in large-dimensional linear and Gaussian state-space models. *IEEE Transactions on Signal Processing*, 63(21):5853–67, 2015.
- B. Ait-El-Fquih and I. Hoteit. A variational Bayesian multiple particle filtering scheme for large-dimensional systems. *IEEE Transactions on Signal Processing*, 64(20):5409–22, 2016.
- B. Ait-El-Fquih and I. Hoteit. A particle-filter based adaptive inflation scheme for the ensemble Kalman filter. *Quarterly Journal of the Royal Meteorological Society*, 147:922–37, 2020.
- B. Ait-El-Fquih and I. Hoteit. *Data Assimilation for Atmospheric, Oceanic and Hydrologic Applications*, volume 4, chapter 3: Filtering with One-Step-Ahead Smoothing for Efficient Data Assimilation. Springer, 2022a. doi: 10.1007/978-3-030-77722-7_3.

- B. Ait-El-Fquih and I. Hoteit. Parallel- and Cyclic-Iterative Variational Bayes for Fast Kalman Filtering in Large-Dimensions. *IEEE Transactions on Signal Processing*, 70:5871–84, 2022b.
- B. Ait-El-Fquih, J.-F. Giovannelli, N. Paul, A. Girard, and I. Hoteit. Parametric Bayesian estimation of point-like pollution sources of groundwater layers. *Signal Processing*, 168:107339, 2020.
- B. Ait-El-Fquih, Aneesh C. Subramanian, and I. Hoteit. A Variational Bayesian Approach for Ensemble Filtering of Stochastically Parametrized Systems. *Quarterly Journal of the Royal Meteorological Society*, 149:1769–88, 2023.
- B. D. O. Anderson and J. B. Moore. *Optimal Filtering*. Prentice Hall, Englewood Cliffs, New Jersey, 1979.
- J. Anderson, T. Hoar, K. Raeder, H. Liu, N. Collins, R. Torn, and A. Avellano. The Data Assimilation Research Testbed: A Community Facility. *Bulletin of the American Meteorological Society*, 90:1283–96, 2009.
- J. L. Anderson. An ensemble adjustment Kalman filter for data assimilation. *Monthly Weather Review*, 129:2884–2903, 2001.
- J. L. Anderson. Exploring the need for localization in ensemble data assimilation using a hierarchical ensemble filter. *Physica D*, 230:99–111, 2007a.
- J. L. Anderson. An adaptive covariance inflation error correction algorithm for ensemble filters. *Tellus*, 59A:210–24, 2007b.
- J. L. Anderson and S. L. Anderson. A Monte Carlo implementation of the nonlinear filtering problem to produce ensemble assimilations and forecasts. *Monthly Weather Review*, 127(12):2741–2758, 1999.
- D.P. Bertsekas. *Nonlinear Programming*. Athena Scientific, Belmont, 1995.
- A. Beskos, D. Crisan, and A. Jasra. On the stability of sequential Monte Carlo methods in high dimensions. *The Annals of Applied Probability*, 24(4):1396–1445, 2014.
- C. H. Bishop and D. Hodyss. Flow-adaptive moderation of spurious ensemble correlations and its use in ensemble-based data assimilation. *Quarterly Journal of the Royal Meteorological Society*, 133:2029–44, 2007.
- C.H. Bishop, B.J. Etherton, and S.J. Majumdar. Adaptive sampling with the Ensemble Transform Kalman Filter. Part I: Theoretical aspects. *Monthly Weather Review*, 129:420–36, 2001.
- D. M. Blei, A. Kucukelbir, and J. D. McAuliffe. Variational inference: A Review for Statisticians. *Journal of the American Statistical Association*, 112:859 – 77, 2017.
- M. Bocquet. Localization and the iterative ensemble Kalman smoother. *Quarterly Journal of the Royal Meteorological Society*, 142:1075–89, 2016.
- G. Burgers, P. Jan van Leeuwen, and G. Evensen. Analysis scheme in the ensemble kalman filter. *Monthly Weather Review*, 126:1719–24, 1998.
- M. A. Chappell, A. R. Groves, B. Whitcher, and M. W. Woolrich. Variational Bayesian Inference for a Nonlinear Forward Model. *IEEE Transactions on Signal Processing*, 57(1):223–36, January 2009.
- D. Crisan and A. Doucet. A survey on convergence results on particle filtering methods for practitioners. *IEEE Transactions on Signal Processing*, 50(3):736–46, 2002.

- M. De La Chevrotière and J. Harlim. A data-driven method for improving the correlation estimation in serial ensemble Kalman filters. *Monthly Weather Review*, 145:985–1001, 2017.
- A. Doucet, S.J. Godsill, and C. Andrieu. On sequential monte carlo sampling methods for Bayesian filtering. *Statistics and Computing*, 10:197–208, 2000.
- C. A. Edwards, A. M. Moore, I. Hoteit, and B. D. Cornuelle. Regional Ocean Data Assimilation. *Annual Review of Marine Science*, 7:21–42, 2015.
- G. Evensen. Sequential data assimilation with nonlinear quasi-geostrophic model using Monte Carlo methods to forecast error statistics. *Journal of Geophysical Research*, 99(C5):143–62, 1994.
- G. Evensen. Sampling strategies and square root analysis schemes for the EnKF. *Ocean Dynamics*, 54:539–60, 2004.
- G. Evensen. *Data Assimilation: The Ensemble Kalman Filter*. New York: Springer, 2006.
- G. Evensen. *Data Assimilation: The Ensemble Kalman Filter*. New York: Springer, 2 edition, 2009.
- E. J. Fertig, B. R. Hunt, E. Ott, and I. Szunyogh. Assimilating non-local observations with a local ensemble Kalman filter. *Tellus A*, 59:719–30, 2007.
- A. Fraysse and T. Rodet. A measure-theoretic variational Bayesian algorithm for large dimensional problems. *SIAM Journal on Imaging Sciences*, 7(4):2591–2622, 2014.
- R. Furrer and T. Bengtsson. Estimation of high-dimensional prior and posterior covariance matrices in Kalman filter variants. *Journal of Multivariate Analysis*, 98(2):227–55, 2007.
- G. Gaspari and S. E. Cohn. Construction of correlation functions in two and three dimensions. *Quarterly Journal of the Royal Meteorological Society*, 125(554):723–757, 1999. ISSN 1477-870X.
- N. J. Gordon, D. J. Salmond, and A. F. M. Smith. Novel approach to nonlinear/ non-Gaussian Bayesian state estimation. *IEE Proceedings - F*, 140:107–113, 1993.
- T. M. Hamill, J. S. Whitaker, and C. Snyder. Distance-dependent filtering of background error covariance estimates in an ensemble Kalman filter. *Monthly Weather Review*, 129:2776–90, 2001.
- I. Hoteit, D.T. Pham, and J. Blum. A simplified reduced order Kalman filtering and application to altimetric data assimilation in Tropical Pacific. *Journal of Marine Systems*, 36(1–2):101–127, 2002.
- I. Hoteit, D-T. Pham, G. Triantafyllou, and G. Korres. A new approximate solution of the optimal nonlinear filter for data assimilation in meteorology and oceanography. *Monthly Weather Review*, 136(1):317–334, 2008.
- I. Hoteit, D.-T. Pham, M. E. Gharamti, and X. Luo. Mitigating observation perturbation sampling errors in the stochastic EnKF. *Monthly Weather Review*, 143:2918–36, 2015.
- I. Hoteit, X. Luo, M. Bocquet, A. Kohl, and B. Ait-El-Fquih. *New Frontiers in Operational Oceanography*, chapter 17: Data assimilation in oceanography: current status and new directions, pages 465–512. GODAE Ocean View, 2018.
- P. Houtekamer and F. Zhang. Review of the ensemble Kalman filter for atmospheric data assimilation. *Monthly Weather Review*, 144:4489–4532, 2016.

- P. L. Houtekamer and H. L. Mitchell. Data assimilation using an ensemble Kalman filter technique. *Monthly Weather Review*, 126:796–811, 1998.
- P. L. Houtekamer and H. L. Mitchell. A sequential ensemble filter for atmospheric data assimilation. *Monthly Weather Review*, 129:123–37, 2001.
- P. L. Houtekamer and H. L. Mitchell. Ensemble Kalman filtering. *Quarterly Journal of the Royal Meteorological Society*, 131:3269–89, 2005.
- C.-C. Hu and P. Jan van Leeuwen. A particle flow filter for high-dimensional system applications. *Quarterly Journal of the Royal Meteorological Society*, 147:2352–74, 2021.
- C.-C. Hu, P. Jan van Leeuwen, and J. L. Anderson. An Implementation of the Particle Flow Filter in an Atmospheric Model. *Monthly Weather Review*, 152:2247–64, 2024.
- B.R. Hunt, E.J. Kostelich, and I. Szunyogh. Efficient data assimilation for spatiotemporal chaos: A local ensemble transform Kalman filter. *Physica D*, 230:112–26, 2007.
- T.S. Jaakkola. Tutorial on variational approximation methods. In M. Opper and D. Saad, editors, *Advanced Mean Field Methods - Theory and Practice*, pages 129–59. MIT Press, 2001.
- T.S. Jaakkola and M.I. Jordan. Bayesian parameter estimation via variational methods. *Statistics and Computing*, 10:25–37, 2000.
- M.I. Jordan, Z. Ghahramani, T.S. Jaakkola, and L.K. Saul. An introduction to variational methods for graphical models. *Machine Learning*, 37:183–233, 1999.
- R. E. Kalman. A new approach to linear filtering and prediction problems. *Transactions of the ASME—Journal of Basic Engineering, Series D*, 82(1):35–45, 1960.
- H. Künsch. State space and hidden markov models. In O. E. Barndorff-Nielsen, D. R. Cox, and C. Klüppelberg, editors, *Complex Stochastic Systems*, chapter 3, pages 109–173. CRC Press, 2001.
- B. Liu, B. Ait-El-Fquih, and I. Hoteit. Efficient Kernel-Based Ensemble Gaussian Mixture Filtering. *Monthly Weather Review*, 144:781–800, 2015.
- Edward N. Lorenz and Kerry A. Emanuel. Optimal sites for supplementary weather observations: Simulation with a small model. *Journal of the Atmospheric Sciences*, 55(3):399–414, 1998.
- X. Luo, T. Bhakta, and G. Nædal. Correlation-based adaptive localization with applications to ensemble-based 4D seismic history matching. *The Society of Petroleum Engineers*, 23:396–427, 2018.
- J. Martens. New insights and perspectives on the natural gradient method. *The Journal of Machine Learning Research*, 1:5753–5828, 2020.
- C. Di Mauro, R. Hostache, P. Matgen, R. Pelich, M. Chini, P. Jan van Leeuwen, N. Nichols, and G. Blöschl. A Tempered Particle Filter to Enhance the Assimilation of SAR-Derived Flood Extent Maps Into Flood Forecasting Models. *Water Resources Research*, 58(8):e2022WR031940, 2022.
- H. L. Mitchell and P. L. Houtekamer. An adaptive ensemble Kalman filter. *Monthly Weather Review*, 128:416–33, 2000.
- T. Miyoshi. The gaussian approach to adaptive covariance inflation and its implementation with the local ensemble transform Kalman filter. *Monthly Weather Review*, 139:1519–35, 2011.

- D.T. Pham. Stochastic methods for sequential data assimilation in strongly nonlinear systems. *Monthly Weather Review*, 129:1194–1207, 2001.
- J. Poterjoy. A Localized Particle Filter for High-Dimensional Nonlinear Systems. *Monthly Weather Review*, 144(1):59–76, 2016.
- R. Potthast, A. Walter, and A. Rhodin. A Localized Adaptive Particle Filter within an Operational NWP Framework. *Monthly Weather Review*, 147(1):345–62, 2019.
- M. Pulido and P. Jan van Leeuwen. Sequential Monte Carlo with kernel embedded mappings: The mapping particle filter. *Journal of Computational Physics*, 396:400 – 15, 2019.
- N. F. Raboudi, B. Ait-El-Fquih, C. Dawson, and I. Hoteit. Combining Hybrid and One-Step-Ahead Smoothing for Efficient Short-Range Storm Surge Forecasting with an Ensemble Kalman Filter. *Monthly Weather Review*, 147:3283–3300, 2019.
- R. Ranganath, D. Tran, and D. M. Blei. Hierarchical variational models. In *Proceedings of the International Conference on Machine Learning*, pages 324 – 33, New York, USA, 2016.
- R. H. Reichle, D. B. McLaughlin, and D. Entekhabi. Hydrologic Data Assimilation with the Ensemble Kalman Filter. *Monthly Weather Review*, 130:103–14, 2002.
- M. Sato. Online model selection based on the variational Bayes. *Neural Computation*, 13(7): 1649–81, July 2001.
- F. Septier and G. W. Peters. *An Overview of Recent Advances in Monte-Carlo Methods for Bayesian Filtering in High-Dimensional Spaces*, chapter 2 : “Theoretical Aspects of Spatial-Temporal Modeling”. SpringerBriefs - JSS Research Series in Statistics, g. w. peters and t. matsui edition, 2015.
- V. Smidl and A. Quinn. *The Variational Bayes Method in Signal Processing*. Springer, 2006.
- V. Smidl and A. Quinn. Variational Bayesian Filtering. *IEEE Transactions on Signal Processing*, 56(10):5020–5030, 2008.
- C. Snyder, T. Bengtsson, P. Bickel, and J. Anderson. Obstacles To High-Dimensional Particle Filtering. *Monthly Weather Review*, 136(12):4629–40, 2008.
- J. S. Whitaker T. M. Hamill and, J. L. Anderson, and C. Snyder. Sigma-point Kalman filter data assimilation methods for strongly nonlinear systems. *Journal of the Atmospheric Sciences*, 66:3498–3500, 2009.
- Michael Tippett, Jeffrey Anderson, Craig Bishop, Thomas Hamill, and Jeffrey Whitaker. Ensemble square root filters. *Monthly Weather Review*, 131(7):1485–1490, 2003.
- D. Urozayev, B. Ait-El-Fquih, I. Hoteit, and D. Peter. A reduced-order variational Bayesian approach for efficient subsurface imaging. *Geophysical Journal International*, 229:838–52, 2022.
- P. Jan van Leeuwen. A consistent interpretation of the stochastic version of the Ensemble Kalman Filter. *Quarterly Journal of the Royal Meteorological Society*, 146:2815–25, 2020.
- H.L. van Trees. *Detection, Estimation, and Modulation Theory : Part I*. John wiley and Sons, New York, 1968.
- X. Wang, C. H. Bishop, and S. J. Julier. Which is Better, an Ensemble of Positive-Negative Pairs or a Centered Spherical Simplex Ensemble? *Monthly Weather Review*, 132(7):1590–1605, 2004.

- J. S. Whitaker and T. M. Hamill. Evaluating methods to account for system errors in ensemble data assimilation. *Monthly Weather Review*, 140:3078–89, 2012.
- J. S. Whitaker and T. S. Hamill. Ensemble Data Assimilation without Perturbed Observations. *Monthly Weather Review*, 130:1913–24, 2002.
- J. S. Whitaker, H. T. Hamill, X. Wei, Y. Song, and Z. Toth. Ensemble data assimilation with the NCEP global forecast system. *Monthly Weather Review*, 136:463–81, 2008.
- Y. Zhang and D. S. Oliver. Improving the ensemble estimate of the Kalman gain by bootstrap sampling. *Mathematical Geosciences*, 42:327–45, 2010.